

PCA-Guided Quantile Sampling: Preserving Data Structure in Large-Scale Subsampling

Foo Hui-Mean and Yuan-chin Ivan Chang

Institute of Statistical Science

Academia Sinica, Taipei, Taiwan 11529

January 13, 2026

Abstract

We introduce Principal Component Analysis-guided Quantile Sampling (PCA-QS), a novel sampling framework designed to preserve both the statistical and geometric structure of large-scale datasets. Unlike conventional PCA, which reduces dimensionality at the cost of interpretability, PCA-QS retains the original feature space while using leading principal components solely to guide a quantile-based stratification scheme. This principled design ensures that sampling remains representative without distorting the underlying data semantics. We establish rigorous theoretical guarantees, deriving convergence rates for empirical quantiles, Kullback–Leibler divergence, and Wasserstein distance, thus quantifying the distributional fidelity of PCA-QS samples. Practical guidelines for selecting the number of principal components, quantile bins, and sampling rates are provided based on these results. Extensive empirical studies on both synthetic and real-world datasets show that PCA-QS consistently outperforms simple random sampling, yielding better structure preservation and improved downstream model performance. Together, these contributions position PCA-QS as a scalable, interpretable, and theoretically grounded solution for efficient data summarization in modern machine learning workflows.

Keywords and Phrases: PCA-guided Quantile Sampling; structure-preserving sampling; quantile stratification; convergence rates; large-scale data reduction.

1 Introduction

The exponential growth of modern datasets poses a fundamental challenge: how to reduce data volume while preserving both statistical fidelity and structural integrity. Conventional sampling strategies, although effective for data reduction, often compromise representativeness, distort key distributions, and degrade the performance of downstream models. To address these limitations, we propose Principal Component Analysis-guided Quantile Sampling (PCA-QS), a principled framework for subsampling that preserves the intrinsic structure of complex datasets.

In contrast to conventional PCA, which projects data into a lower-dimensional subspace—often sacrificing interpretability—PCA-QS retains the full original feature space. Instead, it leverages the leading principal components purely as structural guides to define a quantile-based stratification scheme. Sampling is then conducted within these quantile strata, ensuring that the selected subset faithfully captures major variance patterns, distributional characteristics, and the underlying geometric structure of the data.

The proposed method is supported by rigorous theoretical analysis. By building on established results for empirical quantiles, Kullback–Leibler (KL) divergence, and

Wasserstein distance, we demonstrate that PCA-QS exhibits well-defined convergence behavior: as the sample size grows, the distribution of the sampled subset converges uniformly to that of the full dataset. These guarantees provide a robust theoretical foundation for the method’s representativeness and structural preservation.

PCA-QS makes several notable contributions: First, it introduces a novel sampling paradigm that combines the interpretability of the original feature space with the structural insight provided by principal components. Second, it offers a theoretical framework for parameter selection, including the number of principal components and quantile bins, grounded in explicit convergence rates. Third, it demonstrates empirically—across synthetic and real-world datasets—that PCA-QS consistently outperforms standard simple random sampling (SRS) in maintaining structural fidelity and improving the performance of downstream machine learning models. Finally, it provides a scalable, interpretable, and theoretically justified solution for efficient data summarization in modern machine learning workflows.

The remainder of this paper is organized as follows: Section 2 reviews related work and details the PCA-QS methodology. Section 3 presents empirical evaluations on synthetic and real-world datasets. Section 4 discusses broader implications and concludes the study.

2 Method

Principal Component Analysis (PCA) is a classical technique for dimensionality reduction that projects high-dimensional data onto a lower-dimensional subspace that retains the maximal variance. Given a dataset $\mathbf{X} \in \mathbb{R}^{n \times p}$, the PCA transformation is typically obtained via the Singular Value Decomposition (SVD): $\mathbf{X} = \mathbf{U}\mathbf{D}\mathbf{V}^\top$, where $\mathbf{U} \in \mathbb{R}^{n \times p}$ contains the left singular vectors, $\mathbf{V} \in \mathbb{R}^{p \times p}$ the right singular vectors, and $\mathbf{D} \in \mathbb{R}^{p \times p}$ is a diagonal matrix of singular values. The projection of the dataset onto the top k principal components yields the reduced representation: $\mathbf{Z} = \mathbf{U}_k\mathbf{D}_k$, where \mathbf{U}_k and \mathbf{D}_k contain the first k columns and leading singular values, respectively. While PCA is effective in capturing dominant variance directions, it does not inherently reduce the number of data points. To address this, the PCA-guided Quantile Sampling (PCA-QS) framework augments PCA with a stratified sampling mechanism to achieve both data summarization and structural fidelity.

Property of Quantiles: Let X_1, X_2, \dots, X_n be an i.i.d. sample from a distribution with cumulative distribution function (CDF) $F(x)$. The empirical CDF is defined as $F_n(x) = \frac{1}{n} \sum_{i=1}^n \mathbf{1}(X_i \leq x)$. For a quantile level $p \in (0, 1)$, the true quantile is $q_p = F^{-1}(p)$, and the empirical quantile is $q_p^n = F_n^{-1}(p)$.

By the Glivenko–Cantelli theorem [van der Vaart and Wellner(1996)], the empirical CDF converges uniformly to the true CDF as $n \rightarrow \infty$, i.e., $\sup_x |F_n(x) - F(x)| = O(n^{-1/2})$. Consequently, the quantile estimation error satisfies $q_p^n - q_p = O(n^{-1/2})$.

2.1 PCA-Guided Quantile Sampling Method

Sampling in Principal Component Space: PCA-guided Quantile Sampling (PCA-QS) stratifies data along principal component directions using quantile partitions to facilitate representative sampling. For the case of a single principal component (num. of PCs = 1) and g quantile groups, the data is partitioned into intervals as follows:

$$[\min, Q_1), [Q_1, Q_2), \dots, [Q_{g-1}, \max], \quad (1)$$

ensuring that each group contains an approximately equal proportion of the data.

Quantile Assignment for Multiple Components In the general case with multiple principal components (num. of PCs > 1), quantile stratification extends across a multi-dimensional subspace. For each principal component z_j , the data is divided into quantile bins:

$$\text{Quantile Groups for Component } j : [\text{Min}, Q_1), [Q_1, Q_2), \dots, [Q_{g-1}, \text{Max}].$$

Composite quantile groups are then formed by combining the bin assignments across the selected components. These composite groups are uniquely encoded to facilitate balanced sampling in the reduced PCA space.

Sampling within each composite quantile group is typically random to promote unbiased representation. The number of retained samples per group is defined as:

$$\text{Sample Size per Group} = \min(\lceil \text{retention rate} \times N_g \rceil, N_g),$$

where N_g is the size of the group, and the retention rate controls the overall proportion of retained data. This process preserves both distributional balance and structural integrity. The random selection step may also be replaced by adaptive sampling strategies tailored to downstream tasks.

Before analyzing the theoretical properties of the PCA-QS procedure, we briefly review the relevant convergence characteristics of PCA projections and quantile estimators. A complete procedural description is provided in Appendix ??.

2.2 Large Sample Properties of PCA-QS

Let the population covariance matrix be $\Sigma = \mathbb{E}[(X - \mu)(X - \mu)^T]$, and denote the sample covariance matrix as $\hat{\Sigma} = \frac{1}{n-1} \sum_{i=1}^n (X_i - \bar{X})(X_i - \bar{X})^T$. If $X \sim \mathcal{N}(\mu, \Sigma)$, then $n\hat{\Sigma} \sim \mathcal{W}(\Sigma, n-1)$, where $\mathcal{W}(\cdot, \cdot)$ denotes the Wishart distribution. The estimated eigenvectors \hat{V} of $\hat{\Sigma}$ converge to the true eigenvectors V at the rate $\|\hat{V} - V\|_F = O(n^{-1/2})$.

Now consider the case where only the first principal component is used. Let $Y_i = v_1^T X_i$ for $i = 1, \dots, n$, and suppose the range is partitioned into m quantile bins. Then the number of observations falling into each bin satisfies $n_j = p_j n + O(n^{1/2})$, where p_j is the mass of the true distribution in that bin, yielding a relative error of $(n_j - p_j n) / (p_j n) = O(n^{-1/2})$.

When using the top k components, let $\mathbf{Y}_i = (v_1^T X_i, \dots, v_k^T X_i)$ be the projected scores for sample i . The empirical quantile function over these projections, denoted $q_p^n(\mathbf{Y}, k)$, satisfies the multivariate central limit theorem: $\sqrt{n}(q_p^n(\mathbf{Y}, k) - q_p(\mathbf{Y}, k)) \xrightarrow{d} \mathcal{N}(\mathbf{0}, \Sigma_q(k))$, where $\Sigma_q(k)$ is the asymptotic variance. This leads to the following uniform convergence result:

Theorem 1 (Uniform Convergence of Multiple Quantiles). For any quantile function $q_p^n(\mathbf{Y}, k)$, we have $\sup_p |q_p^n(\mathbf{Y}, k) - q_p(\mathbf{Y}, k)| = O(n^{-1/2})$. This implies that quantiles estimated via PCA-QS converge uniformly across the top k principal components.

Remark 1. This result ensures that PCA-QS preserves statistical representativeness as the sample size increases. See Appendix ?? for an intuitive explanation and visual illustration.

Furthermore, PCA-QS achieves rapid convergence in distributional fidelity. The Kullback–Leibler (KL) divergence between the sampled and full distributions decays at a rate of $O(n^{-1})$, while the Wasserstein distance decays at $O(n^{-1/d})$, reflecting preservation of geometric structure even in high dimensions.

Remark 2. These results imply that as more samples are drawn via PCA-QS, the retained subset becomes increasingly similar to the original data, both statistically and geometrically. See Appendix ?? for conceptual analogies.

Proof of Theorem 1. Let $F_{\mathbf{Y},k}$ be the joint CDF of the top k principal components, and $F_{\mathbf{Y},k}^n(\mathbf{y}) = \frac{1}{n} \sum_{i=1}^n \mathbf{1}(\mathbf{Y}_i \leq \mathbf{y})$ be its empirical estimate. By the Dvoretzky–Kiefer–Wolfowitz (DKW) inequality [Massart(1990)], the uniform error satisfies $\sup_{\mathbf{y}} |F_{\mathbf{Y},k}^n(\mathbf{y}) - F_{\mathbf{Y},k}(\mathbf{y})| = O_p(n^{-1/2})$.

Using the quantile inversion property, we have:

$$F_{\mathbf{Y},k}(q_p^n) - F_{\mathbf{Y},k}(q_p) \approx F_{\mathbf{Y},k}^n(q_p^n) - p = O(n^{-1/2}).$$

Since $F_{\mathbf{Y},k}$ is differentiable with bounded density, the inverse function theorem implies that $|q_p^n - q_p| = O(n^{-1/2})$ for fixed p . Uniform convergence over all $p \in (0, 1)$ then follows by Kolmogorov's uniform law of large numbers, completing the proof. \square

2.3 Distributional Approximation in PCA-QS

Beyond quantile-level accuracy, PCA-QS also achieves strong distributional fidelity. In this section, we examine how the divergence between the empirical and true distributions behaves as the sample size increases.

2.3.1 KL Divergence Decay in PCA-QS

The *Kullback–Leibler (KL) divergence* quantifies how much the empirical distribution P_n , derived via PCA-QS, deviates from the true distribution P . For continuous densities f_n and f , it is defined as:

$$D_{\text{KL}}(f_n \parallel f) = \int f_n(\mathbf{y}) \log \frac{f_n(\mathbf{y})}{f(\mathbf{y})} d\mathbf{y}.$$

To analyze $D_{\text{KL}}(P_n \parallel P)$, let $\mathbf{Y} = (\mathbf{v}_1^T X, \dots, \mathbf{v}_k^T X)$ denote the first k principal components, projecting the original data X into a reduced subspace. The marginal density of \mathbf{Y} , denoted $f_{\mathbf{Y}}$, is given by $f_{\mathbf{Y}}(\mathbf{y}) = \int f_X(\mathbf{x}) d\mathbf{x}_{\perp}$, where \mathbf{x}_{\perp} integrates out the orthogonal complement. Since PCA preserves second-order structure, we assume $f_{\mathbf{Y}}$ is approximately Gaussian.

Let f_n be the kernel density estimator (KDE) of $f_{\mathbf{Y}}$ using the PCA-QS samples. From KDE theory [Silverman(1986)], we have $\sup_{\mathbf{y}} |f_n(\mathbf{y}) - f_{\mathbf{Y}}(\mathbf{y})| = O_p(n^{-1/2})$. Furthermore, the expected L_2 -distance between f_n and f satisfies $\mathbb{E}[\|f_n - f\|^2] = O(n^{-1})$.

Applying *Pinsker's inequality* [Cover and Thomas(2006)], we obtain:

$$D_{\text{KL}}(P_n \parallel P) \leq \frac{1}{2} \mathbb{E} [\|f_n - f\|^2] = O(n^{-1}).$$

This result demonstrates that PCA-QS achieves rapid convergence in KL divergence as the sample size grows. Notably, the rate $O(n^{-1})$ is faster than the quantile convergence rate of $O(n^{-1/2})$, underscoring the strength of PCA-QS in approximating full data distributions under a probabilistic lens.

2.3.2 Wasserstein Distance Decay in PCA-QS

While KL divergence quantifies the discrepancy between probability densities, the *Wasserstein distance* captures geometric differences between distributions. This makes it especially relevant for evaluating how well the spatial structure of data is preserved under sampling.

For probability measures P and P_n on \mathbb{R}^d , the p -Wasserstein distance is defined as:

$$W_p(P_n, P) = \left(\inf_{\gamma \in \Gamma(P_n, P)} \mathbb{E}_{\gamma} [\|\mathbf{y} - \mathbf{y}'\|^p] \right)^{1/p},$$

where $\Gamma(P_n, P)$ is the set of all couplings of P_n and P . For the commonly used case $p = 2$, this simplifies to:

$$W_2(P_n, P) = \left(\inf_{\gamma \in \Gamma(P_n, P)} \mathbb{E}_\gamma [\|\mathbf{y} - \mathbf{y}'\|^2] \right)^{1/2}.$$

Let $\mathbf{Y} = (\mathbf{v}_1^T X, \dots, \mathbf{v}_k^T X)$ be the projection of data X onto its first k principal components, with marginal density $f_{\mathbf{Y}}$ defined by:

$$f_{\mathbf{Y}}(\mathbf{y}) = \int f_X(\mathbf{x}) d\mathbf{x}_\perp.$$

Since PCA preserves the second-order structure of X , PCA-QS samples approximate the distribution of \mathbf{Y} well.

From empirical measure theory and concentration inequalities, $W_2(P_n, P) = O(n^{-1/d})$, where d is the dimension of the space over which the approximation is measured. This rate reflects the well-known curse of dimensionality, where convergence slows in high dimensions. ([Dudley(1999), Boucheron et al.(2013)] [Talagrand(1996), van der Vaart and Wellner(1996)].)

However, PCA-QS mitigates this effect by reducing the effective dimension from d to $k \ll d$. Thus, even though the Wasserstein convergence rate is slower than KL divergence ($O(n^{-1})$), it provides complementary guarantees: KL decay ensures fidelity in density approximation, while Wasserstein decay reflects preservation of geometric structure.

Remark 3. The dual decay rates— $O(n^{-1})$ for KL divergence and $O(n^{-1/d})$ for Wasserstein distance—jointly establish that PCA-QS provides both distributional and spatial fidelity. By operating in a reduced-dimensional space, PCA-QS accelerates convergence and maintains generalization robustness in large-scale settings.

Remark 4 (Comparison of KL Divergence and Wasserstein Distance). KL divergence measures differences in probability densities and decays at a fixed rate of $O(n^{-1})$, ensuring PCA-QS accurately preserves the distributional structure. In contrast, Wasserstein distance quantifies geometric misalignment and decays more slowly at $O(n^{-1/d})$, where d is the dimensionality. However, by projecting data onto a lower-dimensional subspace, PCA-QS effectively reduces d , accelerating Wasserstein convergence. Together, these measures highlight that PCA-QS preserves both probabilistic and geometric fidelity.

2.4 Selection of the Number of Principal Components in PCA-QS

Selecting the number of principal components (k) in PCA-based Quantile Sampling (PCA-QS) is essential for balancing computational cost and fidelity to the original data distribution. The value of k directly influences convergence behavior, including KL divergence decay, Wasserstein stability, and quantile estimation accuracy.

2.4.1 Criteria for Selecting k

PCA transforms data into an orthogonal basis where each component captures a portion of total variance. Let $\lambda_1, \dots, \lambda_d$ be the eigenvalues of the covariance matrix Σ . The cumulative variance explained by the first k components is:

$$\rho_k = \frac{\sum_{j=1}^k \lambda_j}{\sum_{j=1}^d \lambda_j}.$$

A common heuristic is to choose the smallest k such that $\rho_k \geq 0.90$ or 0.95 , ensuring that most variability is retained.

From a distributional perspective, KL divergence decays at rate $D_{\text{KL}}(P_n^{(k)} \| P) = O(k^{-1})$, implying that increasing k enhances density approximation, but with diminishing returns. In contrast, Wasserstein distance decays more slowly as $W_2(P_n^{(k)}, P) = O(n^{-1/k})$, where k acts as the effective dimension. Thus, PCA helps accelerate convergence by reducing $k \ll d$.

Another useful criterion is the spectral gap between eigenvalues, defined as $\lambda_k - \lambda_{k+1}$. A large spectral gap indicates a natural truncation point, beyond which additional components add minimal variance. Selecting k at the largest spectral gap ensures efficient compression without substantial loss.

2.4.2 Cross-Validation Based on Sampling Performance

An alternative is to empirically validate PCA-QS across different k by assessing the mean squared error (MSE) in quantile estimation:

$$\text{MSE}(q_p^n(\mathbf{Y}, k)) = \mathbb{E} [(q_p^n(\mathbf{Y}, k) - q_p(\mathbf{Y}))^2].$$

The optimal k minimizes this error while keeping the dimension low.

Theoretical Justification Choosing an appropriate k ensures that PCA-QS retains critical distributional features. Moderate k values enable fast KL divergence decay for statistical fidelity and reduce effective dimensionality, improving Wasserstein convergence. Spectral gap analysis guards against overfitting to noise by identifying informative components.

Practical Justification In applied settings, computational efficiency often constrains the choice of k . Monitoring when KL divergence stabilizes offers a natural stopping rule. Likewise, Wasserstein distance helps assess spatial consistency in the sampled data. Finally, ensuring that the selected k captures a meaningful share of variance improves interpretability and downstream analysis.

In sum, PCA-QS requires careful selection of k to balance variance retention, distributional convergence, and efficiency. A principled choice of k ensures that PCA-QS remains robust and scalable for large-scale data sampling.

2.5 Balancing Principal Components and Quantiles

In PCA-based Quantile Sampling (PCA-QS), both the number of principal components (k) and the number of quantile bins (m) play a crucial role in determining sampling performance. This section explores their theoretical relationship and offers practical guidance for their selection.

2.5.1 Theoretical Relationship Between k and m

PCA projects data onto a lower-dimensional subspace defined by the top k components, while quantile stratification partitions the projected data into m bins per dimension. The total approximation error in PCA-QS can be decomposed into three sources: sampling error ($O(n^{-1/2})$), projection error ($O(k^{-1})$), and quantile discretization error ($O(m^{-1})$). To minimize the combined error while preserving efficiency, one should balance the projection and discretization terms, i.e., $O(k^{-1}) \approx O(m^{-1})$.

2.5.2 Trade-off Between k and m

Increasing k reduces projection error and better captures data variability, but increases computational cost and necessitates finer stratification (larger m) to preserve detail. Conversely, increasing m refines stratification but requires more data and becomes ineffective if the projection is too coarse (i.e., k too small). Hence, optimal performance depends on jointly tuning these parameters.

Guidelines for Choosing k and m In practice, selection depends on the trade-off between computational efficiency and distributional accuracy. When efficiency is prioritized, a smaller k may be used, with m chosen such that $O(k^{-1}) \approx O(m^{-1})$. For higher fidelity, k should be increased first to reduce projection loss, followed by increasing m to achieve finer stratification. When the sample size n is small, overly large m should be avoided, as sampling error may dominate.

Conclusion Remark The optimal selection of k and m ensures that dimensionality reduction and stratification remain aligned. The guideline $O(k^{-1}) \approx O(m^{-1})$ offers a practical rule for balancing structural integrity and efficiency in PCA-QS.

2.6 Effects of the Number of Quantiles in PCA-QS

The number of quantiles (m) controls the resolution of stratified sampling in PCA-QS. Increasing m refines stratification and improves sampling granularity but also increases computational overhead and risks overfitting, especially with limited data. The quantile approximation error decays as $O(m^{-1})$, yet higher values of m require more samples to ensure empirical stability and meaningful partitions.

In high-dimensional settings, if $m \ll k$, stratification may fail to capture local density variations, degrading sampling quality. Conversely, overly large m with small n results in unstable quantiles due to sparse bins.

Factor	Rate or Condition	Effect on PCA-QS
Quantile Approximation Error $\epsilon_q(k, m)$	$O(m^{-1})$	Finer stratification, better distributional representation
Empirical Quantile Stability q_p^n	$O(n^{-1/2})$	Larger m needs more data to avoid noise
Computational Cost	$O(m \log m)$	Cost of sorting and partitioning increases with m
Quantile Distortion (High Dimensions)	$O(k/m)$	Too few bins ($m \ll k$) can miss local structure
Sampling Bias Reduction	$O(m^{-1})$	More bins reduce bias but may increase variance

Table 1: Influence of Quantile Count m on PCA-QS Performance Metrics

Choosing m should balance stratification resolution with sample size n and dimension k . When n is small, large m may lead to unstable quantiles. In high-dimensional contexts, ensuring that k/m remains bounded avoids excessive quantile distortion. Cross-validation or model-specific performance metrics can help identify an optimal m .

These findings emphasize that PCA-QS performance depends critically on both sample size and quantile selection. Larger samples improve quantile estimation and reduce bias, while KL divergence and Wasserstein distance offer validation metrics for structural fidelity. Section 2.8.1 provides a practical illustration of how to use these theoretical insights to choose optimal PCA-QS parameters.

Remark 5. Instead of relying on random subsampling, PCA-QS partitions data along principal components into quantile-defined groups, ensuring balanced and structure-preserving representation. The formal quantile assignment procedure is detailed in Appendix ??.

2.7 Effect of Sample Size in PCA-QS

This section analyzes how the sample size (n) affects the accuracy, stability, and convergence behavior of PCA-based Quantile Sampling (PCA-QS). Theoretical convergence rates and their implications are summarized in Table 2.

Quantile estimates converge at a rate of $O(n^{-1/2})$, which improves estimation precision slowly. The stability of PCA components also improves at the same rate, yielding more consistent projections. For multi-dimensional stratification using k principal components, uniform quantile convergence remains at $O(n^{-1/2})$, ensuring robust bin assignment as n increases.

In contrast, KL divergence decays faster at $O(n^{-1})$, indicating rapid improvement in distributional approximation. Wasserstein distance decays more slowly at $O(n^{-1/d})$, where d is the data dimension, but this convergence is accelerated by PCA, which reduces the effective dimension.

Factor	Convergence Rate	Impact on PCA-QS
Empirical Quantiles q_p^n	$O(n^{-1/2})$	Accuracy improves gradually with n
PCA Components $\hat{\mathbf{V}}$	$O(n^{-1/2})$	Stability of projections increases
Multiple PCs: $\hat{\lambda}_j, \hat{\mathbf{v}}_j$	$O(n^{-1/2})$	Multi-dimensional quantile robustness improves
Quantile Asymptotic Normality	$\mathcal{N}(\mathbf{0}, \Sigma_q(k))$	Distributional shape stabilizes
Uniform Quantile Convergence	$O(n^{-1/2})$	Consistency across k components
KL Divergence D_{KL}	$O(n^{-1})$	Rapid improvement in distributional match
Wasserstein Distance $W_2(P_n, P)$	$O(n^{-1/d})$	Slower convergence unless PCA is used

Table 2: Impact of Sample Size on PCA-QS Convergence and Sampling Fidelity

In practice, PCA-QS becomes more stable and accurate as n increases. If the primary goal is distributional fidelity, KL divergence provides a sensitive metric due to its faster decay rate. For applications where geometric alignment is critical, monitoring the Wasserstein distance is more appropriate. The sample size also mediates trade-offs between computational cost and statistical precision, making it a key factor in designing scalable and reliable PCA-QS pipelines.

2.8 Practical Guidelines for Applying PCA-QS

Building on the theoretical convergence results and parameter trade-offs discussed in prior sections, this subsection outlines practical considerations for applying PCA-based Quantile Sampling (PCA-QS) effectively. A well-structured application ensures a balance between computational efficiency and statistical accuracy.

Preprocessing and Data Normalization Before applying PCA-QS, the dataset should be standardized — centering each feature to zero mean and scaling to unit variance — to ensure that PCA functions correctly. Handle missing values with appropriate imputation techniques, and examine outliers that could distort the principal components. Proper preprocessing ensures stability in both PCA transformation and quantile stratification.

Choosing the Number of Principal Components (k) Selecting k , the number of retained principal components, is key to preserving structural integrity with minimal complexity. A common approach is to select k such that the cumulative variance explained ρ_k exceeds 90% or 95%. Alternatively, the spectral gap heuristic — selecting k where the eigenvalue drop $\lambda_k - \lambda_{k+1}$ is largest — provides a data-driven cutoff. In high

dimensions, cross-validation may help assess PCA-QS stability across different k values, especially in terms of KL divergence and quantile estimation accuracy.

Selecting the Number of Quantiles (m) for Stratification The number of quantile bins m controls the granularity of stratified sampling. Choosing m too small results in poor resolution, while overly large m introduces variance and computational overhead. To balance projection and stratification errors, set m such that $O(m^{-1}) \approx O(k^{-1})$, aligning the granularity of sampling with the retained PCA detail. Larger values of k necessitate increased m for fidelity, while smaller datasets call for conservative m values to avoid instability.

Schematic of PCA-QS Stratification

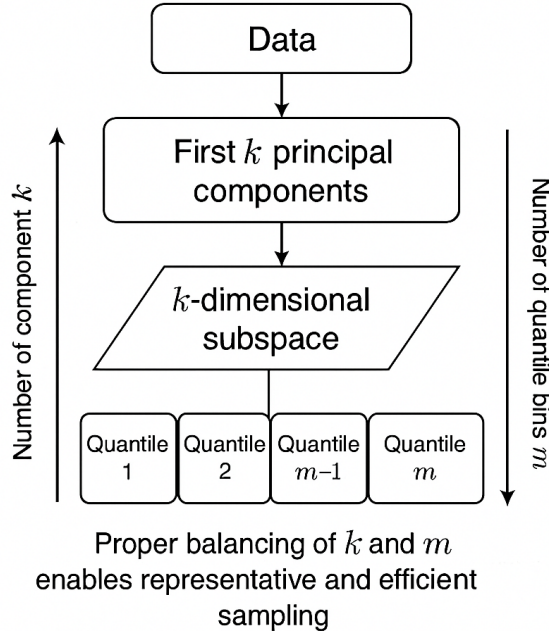


Figure 1: Schematic of PCA-QS stratification. The first k principal components define a subspace in which data are stratified into quantile-based groups. The resolution depends on the number of components and quantile bins. Proper balancing of k and m enables representative and efficient sampling.

Ensuring Distributional Fidelity PCA-QS is designed to maintain both statistical and geometric properties of the dataset. KL divergence decay at $O(n^{-1})$ verifies that the sampled distribution retains key probabilistic features. Meanwhile, Wasserstein distance at $O(n^{-1/d})$ reflects spatial fidelity and benefits from PCA's dimensionality reduction. Evaluating both metrics provides a comprehensive view of distributional accuracy.

Computational Considerations Scalability of PCA-QS is critical for large datasets. Use randomized PCA for approximate decomposition in high dimensions, or incremental PCA in streaming settings. Efficient quantile computation (e.g., Greenwald-Khanna summaries) helps manage stratification overhead. Together, these strategies make PCA-QS feasible in real-world pipelines.

Validating PCA-QS Sampling Performance To confirm performance, compare the empirical quantiles of PCA-QS samples with those of the full dataset. Assess met-

rics such as quantile error, variance retention, and the behavior of KL divergence and Wasserstein distance under sampling. Cross-validation over partitions of the dataset improves robustness by ensuring consistency across subsamples.

PCA-QS provides a flexible and computationally efficient approach to data reduction while preserving distributional structure. Success hinges on selecting k to capture sufficient variance and choosing m to ensure accurate stratification. Validation via multiple distributional metrics ensures that PCA-QS can be confidently deployed for large-scale data analysis.

2.8.1 Example: Optimal Parameter Selection Based on Convergence Rates

To illustrate how theoretical convergence rates guide parameter selection in PCA-based Quantile Sampling (PCA-QS), we consider a hypothetical dataset with $n = 100,000$ samples and $d = 50$ features. The goal is to choose optimal values for the number of principal components k , number of quantile bins m , and the sampling retention rate δ to achieve efficient, structure-preserving subsampling.

Number of Principal Components k The number of components k should capture sufficient variance while limiting computational cost. Let $\rho_k = \sum_{j=1}^k \lambda_j / \sum_{j=1}^d \lambda_j$, where λ_j are eigenvalues of the covariance matrix. We select the smallest k satisfying both:

$$\rho_k \geq V \quad \text{and} \quad k \leq \frac{d}{4}.$$

For $V = 85\%$ and $d = 50$, empirical results suggest $k \in \{12, \dots, 15\}$.

Choosing the Number of Quantiles m The quantile count m should balance projection error $O(k^{-1})$ and quantization error $O(m^{-1})$. A natural guideline is:

$$m \approx \max(k, 15),$$

which for $k = 12-15$, yields $m \in \{15, \dots, 20\}$.

Selecting the Deduction Rate δ The deduction rate controls sampling intensity. KL divergence decays rapidly as $O(n^{-1})$, allowing for aggressive reduction, whereas Wasserstein distance $O(n^{-1/d})$ requires more cautious downsampling to preserve geometry. For large n , empirical evidence supports:

$$\delta = 0.05 \quad (\text{default}), \quad \delta = 0.10 \quad (\text{for higher fidelity}).$$

Computational Considerations The full cost includes PCA computation $O(ndk)$ (or $O(nd)$ for randomized PCA), quantile sorting $O(n \log m)$, and sampling $O(n)$. For large-scale applications, Incremental PCA or Randomized PCA, and efficient quantile estimation (e.g., Greenwald–Khanna) are recommended.

Summary of Recommended Parameters Using the above criteria, the recommended parameters for the given dataset are:

$$k = \min \left\{ \arg \min_k (\rho_k \geq V), \frac{d}{4} \right\}, \quad m = \max(k, 15), \quad \delta \in \{0.05, 0.10\}.$$

For $d = 50$ and $V = 85\%$, we obtain $k \in \{12, \dots, 15\}$, $m \in \{15, \dots, 20\}$, and $\delta = 0.05$ (or 0.10 for more precision).

PCA-QS Parameter Selection as a Trade-Off Optimization Parameter tuning in PCA-QS can be viewed as a constrained optimization that balances distributional fidelity and computational efficiency. Projection error decays at rate $O(k^{-1})$, while quantile approximation error decays as $O(m^{-1})$, suggesting that m should scale roughly with k . KL divergence decays faster at $O(n^{-1})$, allowing for aggressive data reduction via small δ , whereas Wasserstein distance decays more slowly at $O(n^{-1/d})$, benefiting from dimension reduction through PCA.

In practice, heuristics such as setting $m \approx k$ and choosing $\delta \in [0.05, 0.10]$ perform well across many settings. Nonetheless, in high-dimensional or small-sample scenarios, data-specific tuning may yield further improvements. This underscores the value of adaptive strategies for optimizing PCA-QS parameters in applied settings.

For a detailed derivation of the quantile assignment and optimization of parameter settings, please refer to the Supplementary Material.

3 Numerical Study

3.1 Synthesized Data

Properties of Retentive Data Sets This section evaluates how well *PCA-based Quantile Sampling (PCA-QS)* and *Simple Random Sampling (SRS)* preserve the statistical structure of high-dimensional data. Specifically, we examine their ability to retain covariance structure and distributional properties relative to the full dataset.

We simulate a synthetic dataset with 100,000 samples and 50 features using a block-wise correlated covariance matrix, optionally enhanced with a Gaussian Mixture Model (GMM) to test robustness under multimodal structures.

PCA-QS is applied with a retention rate of $\delta = 0.05$, using quantile binning over several principal components. SRS selects samples uniformly without regard to structure. We compare both sampling strategies using geometric and probabilistic distance metrics. Technical details of the PCA-QS stratification procedure are provided in the Supplementary material.

Quantitative Comparison of Covariance and Distributional Distances We compare the performance of *PCA-based Quantile Sampling (PCA-QS)* and *Simple Random Sampling (SRS)* across different numbers of retained principal components: 3, 5, 10, and a dynamic choice based on preserving 70% of cumulative variance. Each sampling method produces a reduced dataset, which is evaluated against the original data using similarity metrics such as covariance fidelity, KL divergence, and Wasserstein distance. Results are averaged over 1,000 replications for each configuration to ensure statistical stability.

Synthetic Data Generation

The synthetic data are constructed for binary classification using a structured Gaussian mixture model. Each instance consists of a feature vector $x \in \mathbb{R}^{30}$ and a class label $y \in \{0, 1\}$, with a class imbalance of 90:10. The 30-dimensional feature space includes 20 informative variables that are statistically dependent on the label, 5 redundant variables formed as linear combinations of the informative ones, 2 repeated copies, and 3 pure noise variables drawn independently from standard normal distributions.

Class-conditional informative features are sampled as $x_{y=0}^{(\text{inf})} \sim \mathcal{N}(\mu_0, I)$ and $x_{y=1}^{(\text{inf})} \sim \mathcal{N}(\mu_1, I)$, where $\|\mu_1 - \mu_0\| = 1.5 \cdot \sqrt{20} \approx 6.7$. This structure ensures a moderate separation between the classes while introducing dependencies and noise that resemble

real-world data. The full dataset contains one million samples and is standardized to zero mean and unit variance prior to sampling.

This experimental design provides a controlled setting for assessing how well SRS and PCA-QS retain the statistical and geometric structure of the original data under various sampling configurations.

Quantitative Comparison of Covariance and Distributional Distances We compare the performance of *PCA-based Quantile Sampling (PCA-QS)* and *Simple Random Sampling (SRS)* across different numbers of retained principal components: 3, 5, 10, and a dynamic choice based on preserving 70% of cumulative variance. Each sampling method produces a reduced dataset, which is evaluated against the original data using similarity metrics such as covariance fidelity, KL divergence, and Wasserstein distance. Results are averaged over 1,000 replications for each configuration to ensure statistical stability.

Evaluation For PCA-QS, the principal component projections are computed using **Truncated SVD**, a scalable PCA variant well-suited for high-dimensional or sparse data. We consider both fixed numbers of principal components (3, 5, and 10) and a dynamic configuration where the number of components is chosen to explain at least 70% of total variance. Each retained component is divided into $Q = 10$ quantile bins, and stratified sampling is performed across these bins to preserve the structure of the projected space.

To assess how well the sampled subsets approximate the full dataset, we employ a set of statistical and geometric distance metrics. These include: (i) the *Jensen-Shannon (JS) divergence*, defined as $JS(P\|Q) = [\text{KL}(P\|M) + \text{KL}(Q\|M)]/2$, where $M = (P+Q)/2$; (ii) the *Kullback-Leibler (KL) divergence*, $\text{KL}(P\|Q) = \sum_i P(i) \log \frac{P(i)}{Q(i)}$; (iii) the *Energy Distance*, given by $D_E(X, Y) = 2\mathbb{E}\|X - Y\| - \mathbb{E}\|X - X'\| - \mathbb{E}\|Y - Y'\|$; (iv) the *Maximum Mean Discrepancy (MMD)*, where $\text{MMD}^2 = \mathbb{E}[k(x, x')] + \mathbb{E}[k(y, y')] - 2\mathbb{E}[k(x, y)]$ with an RBF kernel $k(x, y) = \exp(-\gamma\|x - y\|^2)$ with $\gamma = 1.0$; (v) the *Mahalanobis Distance*, computed as $D_M(x, \mu, \Sigma) = \sqrt{(x - \mu)^T \Sigma^{-1} (x - \mu)}$; and (vi) a *Pairwise Distance Difference* metric, defined as the average absolute difference between all pairwise distances in the original and sampled datasets:

$$\frac{1}{n(n-1)} \sum_{i \neq j} \left| D_{ij}^{\text{orig}} - D_{ij}^{\text{proj}} \right|,$$

where D_{ij}^{orig} and D_{ij}^{proj} denote the pairwise distances between samples i and j in the full and sampled datasets, respectively. These complementary metrics offer a comprehensive evaluation of how well SRS and PCA-QS preserve both distributional and geometric properties of the original data.

Figure 2 presents box-plots of each metrics for PCA-QS and SRS. Each box-plot provides a visual distribution of metric values over 1000 runs, stratified by the setting of PC's. Figures demonstrate clear, consistent trends: For every metric, PCA-QS has narrower IQRs (inter-quartile range) and lower medians, visually reinforcing its statistical robustness. SRS results are more dispersed, particularly at low PC settings, confirming its sensitivity and stochastic inconsistency.

Figure 2a shows the Jensen-Shannon Divergence (JS Divergence), which measures the similarity between label distributions in the retained datasets. PCA-QS showed near-zero values across all PC settings, indicating high preservation of label distribution. SRS had significantly higher JS divergence, reflecting inconsistency and loss in label similarity. Figure 2b presents box-plots for energy distance – a metric based on

the statistical distribution of distances. PCA-QS had consistently lower values, while SRS showed large fluctuations and higher energy distances, indicating less structural preservation. Figure 2c is Kullback-Leibler divergence (KL Divergence), which is a commonly used probabilistic measure of divergence between distributions. KL divergence for PCA-QS remained close to zero, suggesting minimal distortion. SRS values were significantly large, implying substantial information loss. Maximum mean discrepancy (MMD) quantifies distributional similarity in terms of means of feature mappings. In Figure 2d, we see that PCA-QS yielded extremely low MMD values, demonstrating almost no change in underlying data distributions. SRS was again consistently higher and fixed, suggesting less robustness in selection. We use Mahalanobis distance to evaluate the distance between distributions considering correlations. Figure 2e shows that PCA-QS had more consistent Mahalanobis distances, whereas SRS exhibited more variability. Figure 2f is distance difference is used to assess average pairwise distance differences between original and retained datasets. PCA-QS again performed better, maintaining closer distance profiles to the original data. SRS showed greater variance, especially for low PC settings like 3 and 5.

Although PCA-QS outperforms SRS in distributional and divergence-based metrics (JS, KL, MMD, Energy), it incurs slightly higher average distance distortion. This suggests a trade-off: PCA-QS better preserves overall structure and class distributions, while SRS may retain local distances more faithfully.

Table 3: Comparison of PCA-QS and SRS across PC Settings using various statistical similarity metrics.

PCs	Metric	PCA-QS	SRS	p-value
3	Jensen-Shannon	0.0001 (0.0002)	0.0449 (0.0376)	1.02e-193
	Distance Difference	1.5462 (0.0382)	1.0152 (0.4601)	1.68e-185
	Energy Distance	0.0684 (0.0057)	6.4367 (0.7005)	0
	Kullback-Leibler	0.1972 (0.0111)	18.4693 (0.1427)	0
	Maximum Mean	0.0067 (0.0000)	0.6667 (0.0000)	0
	Mahalanobis Distance	9.1905 (0.0317)	8.9954 (0.5860)	1.11e-24
5	Jensen-Shannon	0.0000 (0.0000)	0.0308 (0.0203)	2.46e-261
	Distance Difference	1.5349 (0.0370)	1.2217 (0.3462)	9.93e-132
	Energy Distance	0.0660 (0.0056)	4.1291 (0.5101)	0
	Kullback-Leibler	0.0332 (0.0040)	17.1552 (0.1638)	0
	Maximum Mean	0.0067 (0.0000)	0.4000 (0.0000)	0
	Mahalanobis Distance	9.1997 (0.0029)	8.9671 (0.4555)	2.76e-52
10	Jensen-Shannon	0.0000 (0.0000)	0.0187 (0.0186)	1.16e-154
	Distance Difference	1.5395 (0.0357)	1.3877 (0.2359)	1.66e-75
	Energy Distance	0.0656 (0.0049)	2.0787 (0.2465)	0
	Kullback-Leibler	0.0000 (0.0000)	14.6066 (0.2142)	0
	Maximum Mean	0.0067 (0.0000)	0.2000 (0.0000)	0
	Mahalanobis Distance	9.1922 (0.0006)	9.0769 (0.3227)	6.15e-28
dyn=21	Jensen-Shannon	0.0000 (0.0000)	0.0074 (0.0108)	3.13e-84
	Distance Difference	1.5406 (0.0367)	1.4679 (0.1441)	3.76e-49
	Energy Distance	0.0685 (0.0045)	0.8208 (0.0873)	0
	Kullback-Leibler	0.0000 (0.0000)	10.3052 (0.2723)	0
	Maximum Mean	0.0067 (0.0000)	0.0952 (0.0000)	0
	Mahalanobis Distance	9.1917 (0.0005)	9.2239 (0.2181)	3.42e-06

Remark 6. PCA-QS actually shows higher Distance Difference values than SRS in all

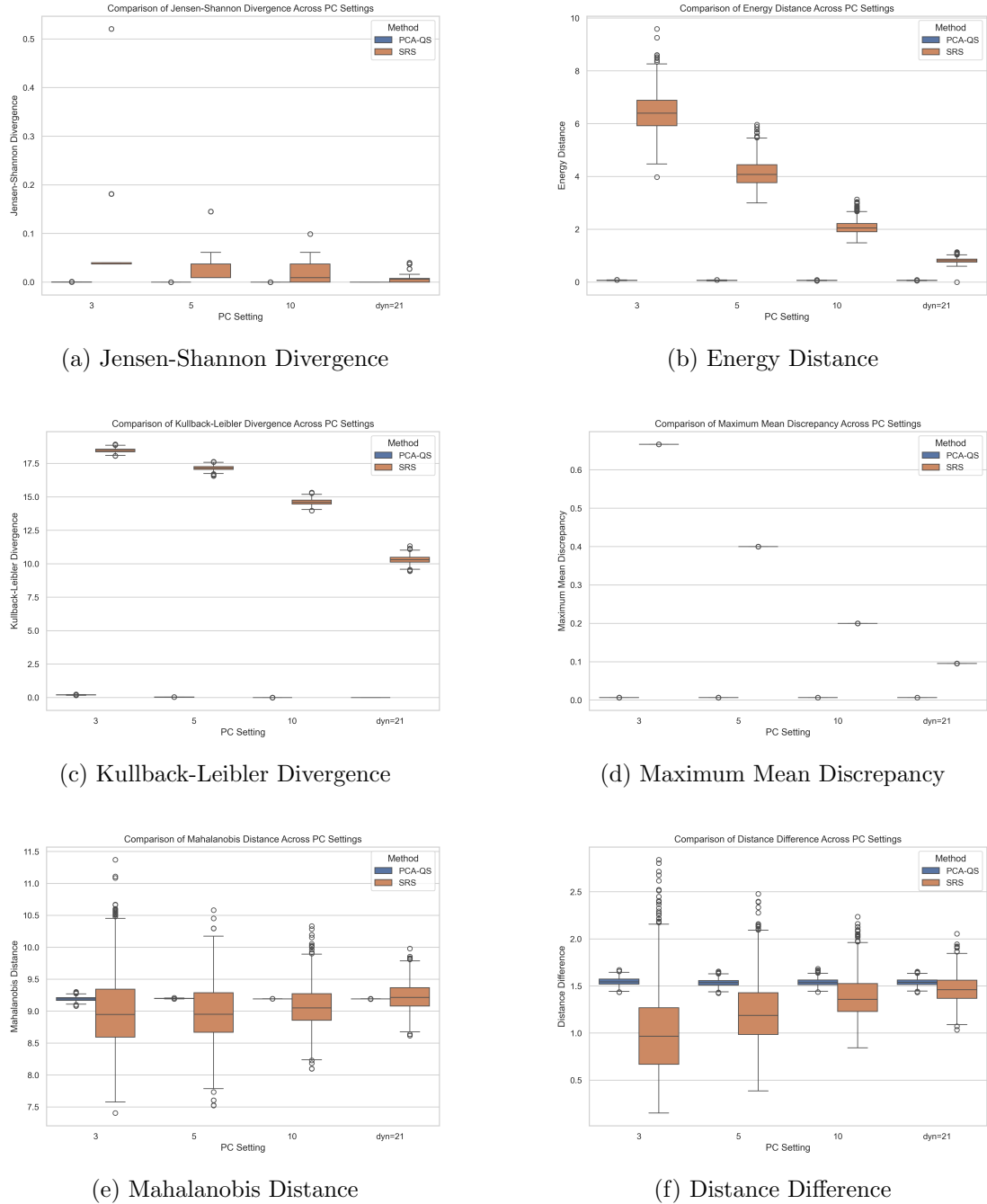


Figure 2: Comparison of PCA-QS and SRS across PC Settings using various statistical similarity metrics.

PC settings. This contradicts the general trend observed in other metrics, where QS was consistently better. It is because while PCA-QS preserves global structure and distributions (as shown by low JS, KL, MMD), it may distort pairwise distances slightly more than SRS. This could stem from the dimensional compression in PCA, which sacrifices some fine-grained inter-point relationships to retain global variance. SRS retains actual points, hence it may better preserve exact distances — even though it loses higher-level structure.

3.1.1 Logistic Regression with Synthesized Data

This experiment evaluates the effectiveness of PCA-based Quantile Sampling (PCA-QS) versus Simple Random Sampling (SRS) in preserving predictive structure for supervised learning. We use logistic regression on a synthetic dataset designed to exhibit complex feature interactions and imbalanced class distributions.

Data Generation We simulate a binary classification task using a two-component Gaussian Mixture Model (GMM). The input matrix $X \in \mathbb{R}^{n \times d}$ contains $n = 100,000$ samples and $d = 50$ features, with class labels $y \in \{0, 1\}^n$ drawn from a Bernoulli distribution with class priors $P(y = 0) = 0.9$, $P(y = 1) = 0.1$. The class-conditional distributions are:

$$X \mid y = 0 \sim \mathcal{N}(\mathbf{0}, \mathbf{I}), \quad X \mid y = 1 \sim \mathcal{N}(0.5 \cdot \mathbf{1}, 1.2 \cdot \mathbf{I}),$$

where $\mathbf{I} \in \mathbb{R}^{50 \times 50}$ is the identity matrix.

To emulate nonlinear and interaction effects, we augment each feature vector with: (1) All pairwise interaction terms $x_i x_j$, for $i < j$, yielding $\binom{50}{2} = 1225$ features, and (2) Sine-transformed features $\sin(x_i)$, adding 50 features. This results in a final dimensionality of $d_{\text{final}} = 1325$.

Sampling Strategy From the full dataset, a subset of 5000 samples is drawn using either PCA-QS or SRS. PCA-QS involves projecting data onto the top principal components that retain at least 70% of total variance, followed by stratified sampling across 10 quantile bins formed from the PCA scores. To reduce sampling noise, nearest-neighbor smoothing with $k = 5$ is optionally applied during bin assignment. A test set of 1000 independent samples is reserved for model evaluation. All experiments use fixed random seeds for reproducibility.

Sampling and Classification Strategy: For SRS, training samples are drawn uniformly at random from the full dataset. For PCA-QS, the procedure involves three steps: (1) applying PCA to the normalized data matrix, (2) discretizing the top principal components into quantile bins, and (3) performing stratified sampling across these composite quantile groups to ensure proportional coverage in the reduced PCA space.

To assess predictive performance, we apply five widely used classifiers to the retentive subsets obtained via PCA-QS and SRS: `logistic regression`, `k-nearest neighbors (kNN)`, `random forest (RF)`, `support vector machine (SVM)`, and `Extreme Gradient Boosting (XGBoost)`. Each model is trained on a sample of 5,000 observations and evaluated on a held-out test set of 1,000 observations. Classification performance is measured using multiple evaluation metrics: accuracy, area under the ROC curve (AUC), F1 score, true positive rate (TPR), false positive rate (FPR), true negative rate (TNR), and false negative rate (FNR). These metrics offer complementary perspectives on classification effectiveness under balanced and imbalanced class conditions.

The following box-plots provide some visual Comparison. Figures 3 and 4 show the box-plots of commonly used classification metrics – accuracy, AUC, F1m true positive rate (TPR), true negative rate (TNR), false positive rate (FPR) and false negative rate (FNR). From these box-plots, we can see that the methods with PCA-QS data set consistently outperform the methods with SRS samples.

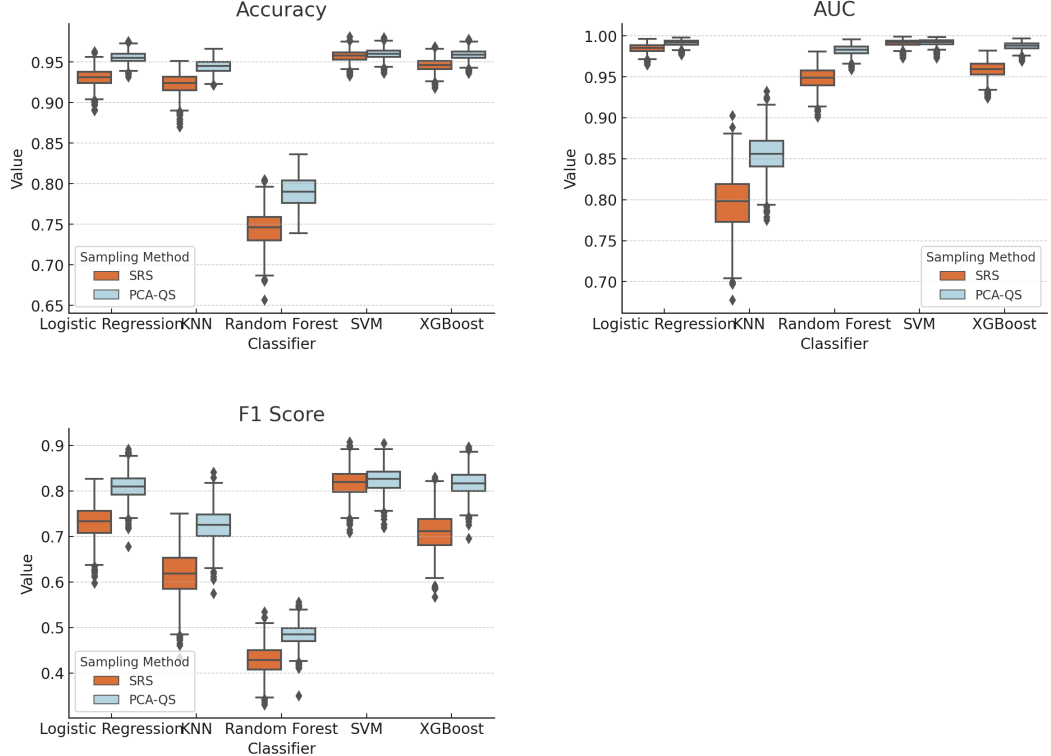


Figure 3: Visual comparison of Accuracy, AUC, and F1 Score across classifiers (Logistic Regression, KNN, Random Forest, SVM, XGBoost). PCA-QS typically yields higher or more stable results, particularly for AUC and F1 metrics.

Summary of Results This study compares PCA-based Quantile Sampling (PCA-QS) and Simple Random Sampling (SRS) across five classifiers: logistic regression, KNN, random forest, SVM, and XGBoost, using synthetic datasets with correlated feature structures. Classification performance was evaluated using accuracy, AUC, F1-score, and confusion-matrix-based metrics, including true positive rate (TPR), true negative rate (TNR), false positive rate (FPR), and false negative rate (FNR).

Results show that PCA-QS consistently outperforms SRS across most classifiers and metrics. It delivers higher AUC and F1 scores, especially for KNN, random forest, and XGBoost. Additionally, PCA-QS achieves better TPR and TNR, and lower FPR and FNR. Standard deviations across replications are also smaller, highlighting its stability. These improvements are statistically significant, with most p-values below 0.001.

The effectiveness of PCA-QS comes from its stratified sampling in the PCA-transformed space. Unlike the uniform randomness of SRS, PCA-QS ensures representation across the principal components, capturing structural variation more reliably. This helps improve both generalization and representativeness, especially in high-dimensional or heterogeneous data scenarios.

In summary, PCA-QS is a robust and efficient subsampling technique that preserves essential data characteristics and enhances classification performance, making it a strong

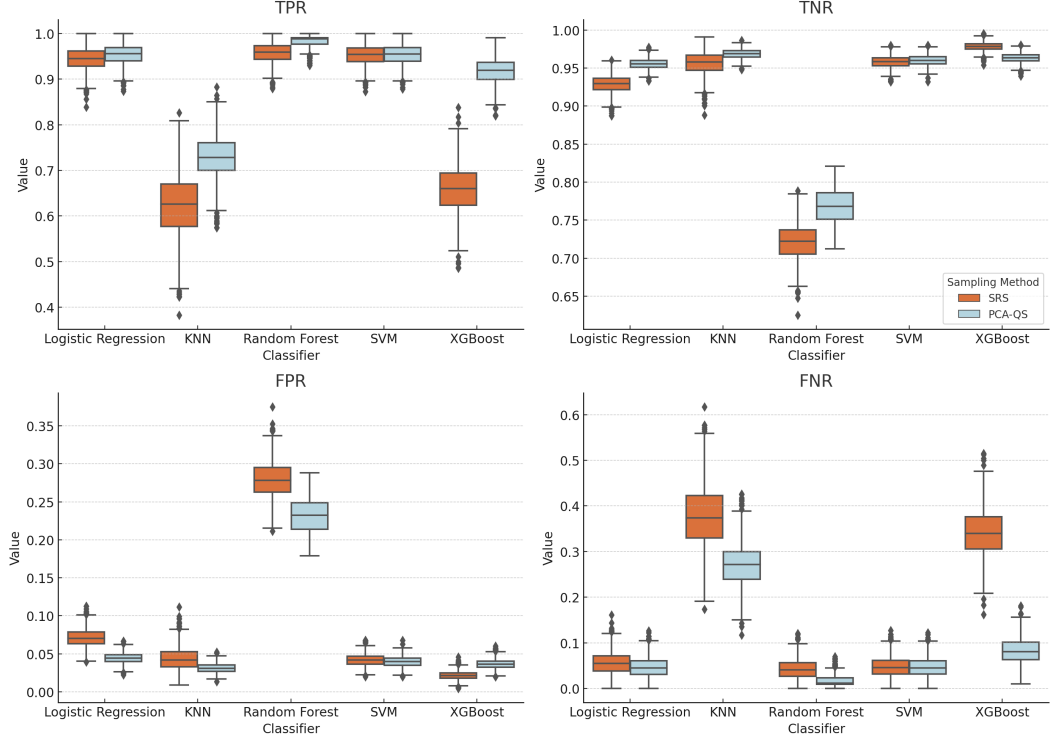


Figure 4: Comparison of TPR, TNR, FPR, and FNR distributions. PCA-QS improves sensitivity and specificity across classifiers, reducing false positive and false negative rates.

alternative to traditional random sampling. We also include a python code for logistic regression with synthesized data in Supplementary material

Remark 7. The choice of PCA-QS parameters should reflect the goal of the application. If computational efficiency is the main concern, a higher deduction rate of 2–5%, a smaller number of principal components (around 6 to 10), and 10 to 15 quantile groups are often sufficient. For statistical representativeness, more variance should be retained—typically 85% to 95%—by selecting 12 to 15 components and 15 to 20 quantile bins. When geometric preservation is important, such as in clustering or anomaly detection, 12 to 20 components and 20 to 30 quantiles can better maintain local structure. If interpretability is the goal, fewer components (around 6 to 10) and a slightly lower variance threshold (80% to 85%) keep the reduced data more understandable. In large-scale or real-time applications, a moderate setup—such as 8 to 12 components, 10 to 15 quantiles, and a 2–5% deduction rate—offers a balanced trade-off between efficiency and accuracy.

Overall, PCA-QS is adaptable and should be configured based on the analysis objectives. Its flexibility allows it to be tailored to different domains while maintaining both computational and statistical integrity.

3.2 Recommended Settings and Consistency

Our empirical results align closely with the theoretical convergence guarantees of PCA-QS. Across diverse datasets and tasks, PCA-QS consistently achieves lower distributional distances (KL divergence, Energy distance, Mahalanobis distance, and MMD) than simple random sampling (SRS). The advantage is more pronounced in higher-dimensional settings, demonstrating its effectiveness in mitigating the curse of dimensionality. Em-

empirical tests confirm that selecting 12–15 principal components captures sufficient variance and achieves strong performance, consistent with theoretical recommendations. Larger sample sizes reduce divergence at the expected rate (e.g., KL decay of $O(n^{-1})$), and using 15–20 quantile groups provides a practical balance between local structure preservation and computational cost. A deduction rate of 5–10% reliably maintains representativeness while significantly reducing data size.

Recommended parameter choices based on both theory and empirical validation are as follows: (1) Principal components (k): 12–15, (2) Quantile groups (m): 15–20, (3) Deduction rate (δ): 5–10%, and (4) Minimum sample size (n): at least 1000.

These settings provide a practical default for practitioners seeking a good trade-off between computational efficiency and statistical fidelity. Detailed derivations and extended results are available in the supplementary appendix.

3.3 Real Data: Thematic Comparison:Structure Preserving of Retentive Data Sets

3.3.1 Imbalanced Datasets

CreditCard The UCI Credit Card dataset is a well-known dataset for binary classification tasks related to credit risk assessment. It contains data on credit card clients in Taiwan and is primarily used to predict whether a client will default on their payment in the next month. The dataset includes 30,000 instances, each representing an individual client, with 23 features capturing demographic information (such as age, gender, and education), credit history (such as past payment behavior), and billing information over six months. The target variable is binary, indicating whether the client defaulted on the next month’s payment (1) or not (0). All features are numerical, though some represent categorical concepts encoded as integers. This dataset is widely used in financial analytics, fraud detection, and machine learning research focused on imbalanced classification problems and model interpretability in credit scoring systems.

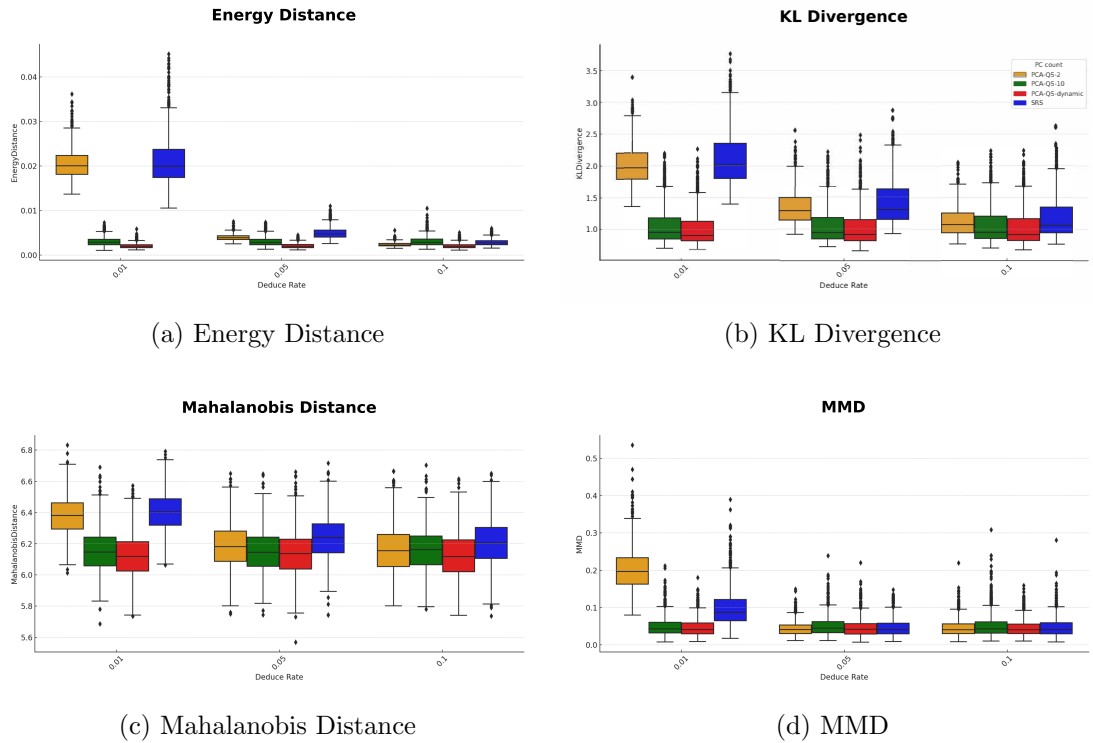


Figure 5: UCI Credit Card Dataset

Magic Gamma Telescope The MAGIC Gamma Telescope dataset from the UCI Machine Learning Repository is designed for binary classification tasks related to high-energy astrophysics. It simulates data from a ground-based atmospheric Cherenkov gamma telescope, aiming to distinguish between gamma rays (signal) and hadronic cosmic rays (background noise) based on the characteristics of particle showers in the atmosphere. Each instance in the dataset represents an event and includes 10 numerical features derived from the image parameters of the recorded showers, such as length, width, size, and conciseness. The target variable is categorical, indicating whether the event is a gamma ray or a hadron. The dataset contains 19,020 instances, with all features being continuous and real-valued. It is widely used for testing classification algorithms, especially in the context of imbalanced datasets, as the two classes are not evenly distributed. This dataset provides a practical scenario for machine learning applications in physics and signal detection.

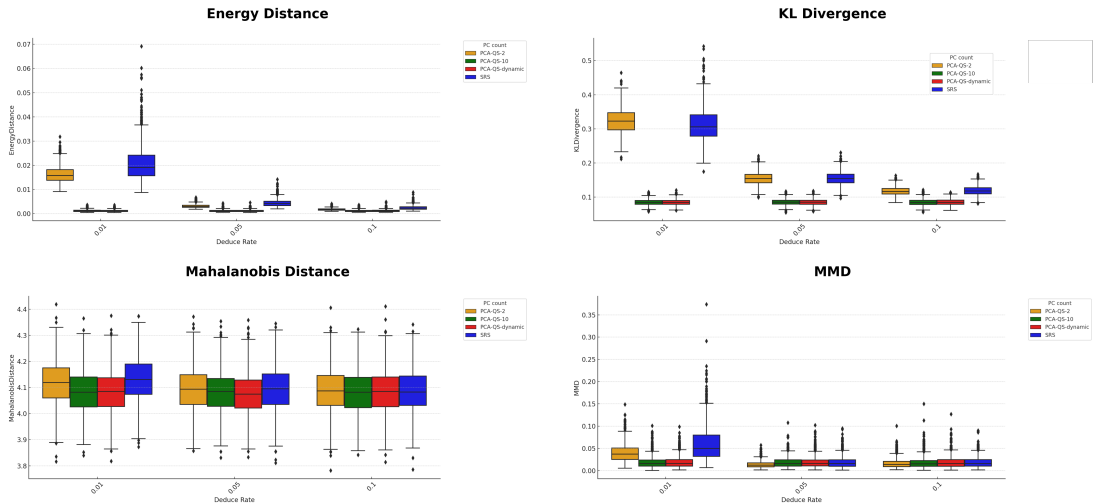


Figure 6: Distance Metrics for Two Sampling Methods with Magic Gamma Telescope Data

3.3.2 Time-Series and Signal Data

Epileptic Seizure Recognition The Epileptic Seizure Recognition dataset from the UCI Machine Learning Repository is designed for multiclass classification tasks related to the detection of epileptic seizures using EEG (electroencephalogram) signals. Each instance in the dataset represents a 1-second segment of EEG data, recorded using a single electrode from a patient. The data is preprocessed into 178 time-ordered measurements per segment, along with one target label. The target variable includes five classes, where class 1 represents seizure activity and classes 2 through 5 represent different non-seizure states recorded during various normal activities. The dataset contains 11,500 instances, each with 178 numerical features and one categorical label. This dataset is widely used in biomedical signal processing and machine learning applications focused on neurological disorder detection, offering a clean, high-dimensional, and balanced example for time-series classification problems.

EEG Eye State The EEG Eye State dataset from the UCI Machine Learning Repository is used for binary classification tasks involving the detection of a person’s eye state—whether open or closed—based on EEG (electroencephalogram) signals. The data was collected from one participant using an Emotiv EEG headset with 14 sensors

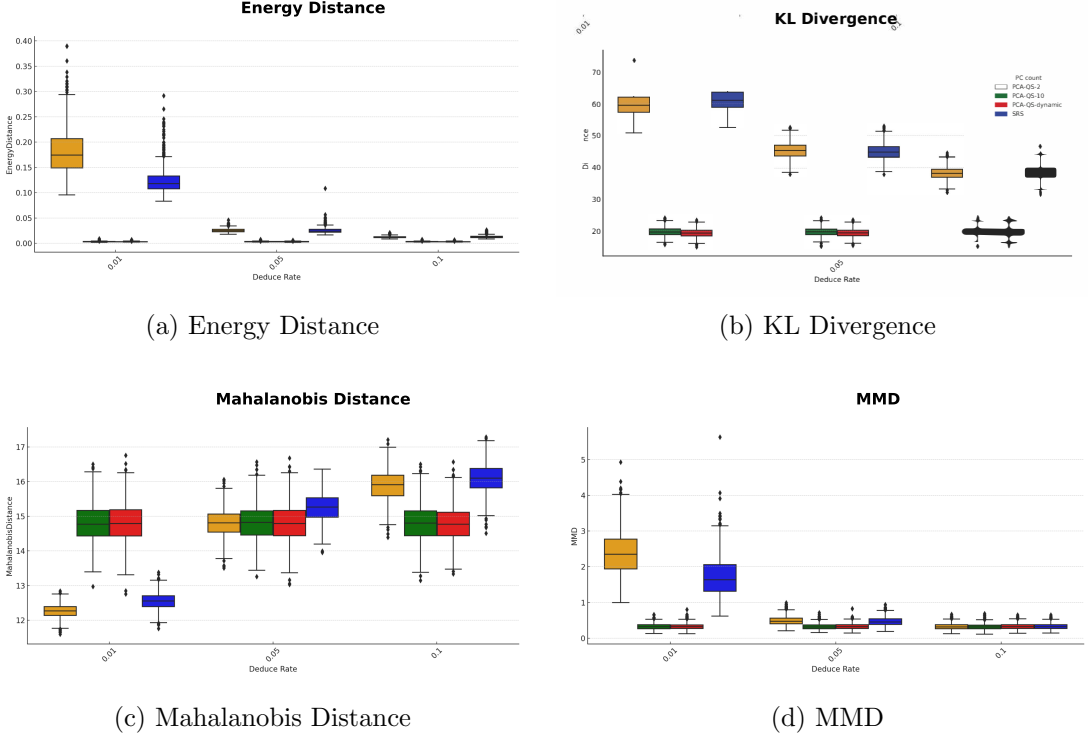


Figure 7: Epileptic Seizure Dataset

while performing normal daily activities. Each instance includes 14 continuous numerical features corresponding to the EEG readings from the sensors, along with a binary target variable: 0 for eyes open and 1 for eyes closed. The dataset contains 14,980 instances in total. It is commonly used to test real-time brain-computer interface applications, signal processing models, and lightweight classification algorithms suitable for wearable or embedded systems.

3.3.3 Large-Scale Tabular Data

Higgs Data set The HIGGS dataset from the UCI Machine Learning Repository is a large-scale benchmark dataset created for binary classification tasks in high-energy particle physics. It simulates the process of distinguishing between signal events that originate from the decay of a Higgs boson and background events that do not. Each instance represents a collision event and includes 28 numerical features: 21 low-level kinematic properties measured directly by the particle detectors, and 7 high-level features derived from those measurements through complex physics calculations. The target variable is binary, indicating whether the event corresponds to a Higgs boson (signal) or not (background). The dataset contains 11 million instances in total, making it suitable for testing the scalability and performance of machine learning models on very large datasets. It has become a popular benchmark for deep learning and large-scale classification research, especially in scientific computing contexts where interpretability and computational efficiency are critical.

Year Prediction MSD The YearPredictionMSD dataset from the UCI Machine Learning Repository is a large-scale benchmark dataset used for regression tasks, specifically aimed at predicting the release year of songs based on their audio characteristics. It is derived from the Million Song Dataset and contains 515,345 instances, each representing a song. Each instance includes 90 numerical audio features extracted from signal

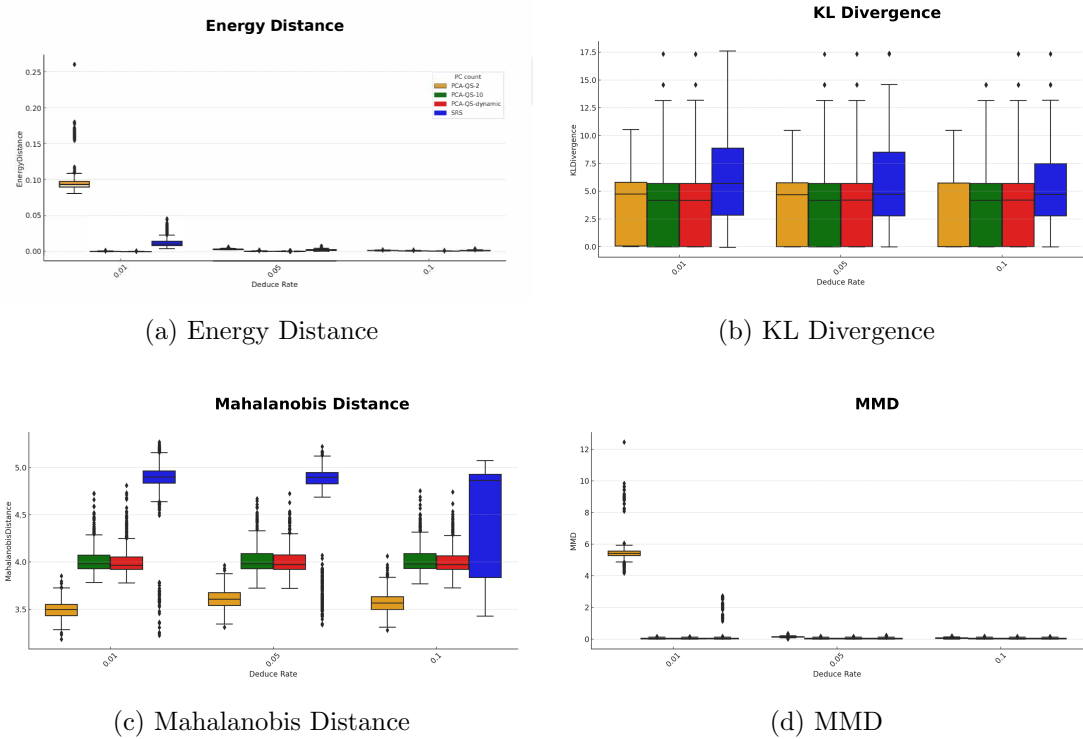


Figure 8: EEG Eye State Dataset

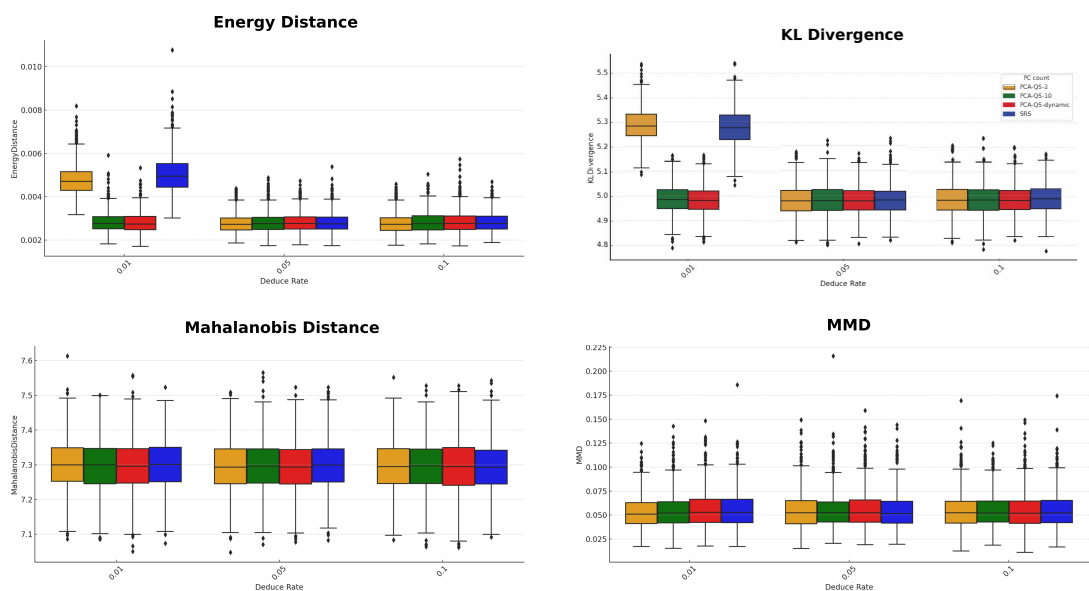


Figure 9: Distance Metrics for Two Sampling Methods with Higgs Data

processing techniques, such as timbre averages and covariances. The first column in each row is the target variable, which is the year the song was released, while the remaining columns are the input features. All data are continuous and numerical. The dataset is split into a training set with 463,715 samples and a test set with 51,630 samples. This dataset is frequently used to benchmark regression models and study high-dimensional, real-world data in the context of music analysis and machine learning. It is available at the UCI Machine Learning Repository.

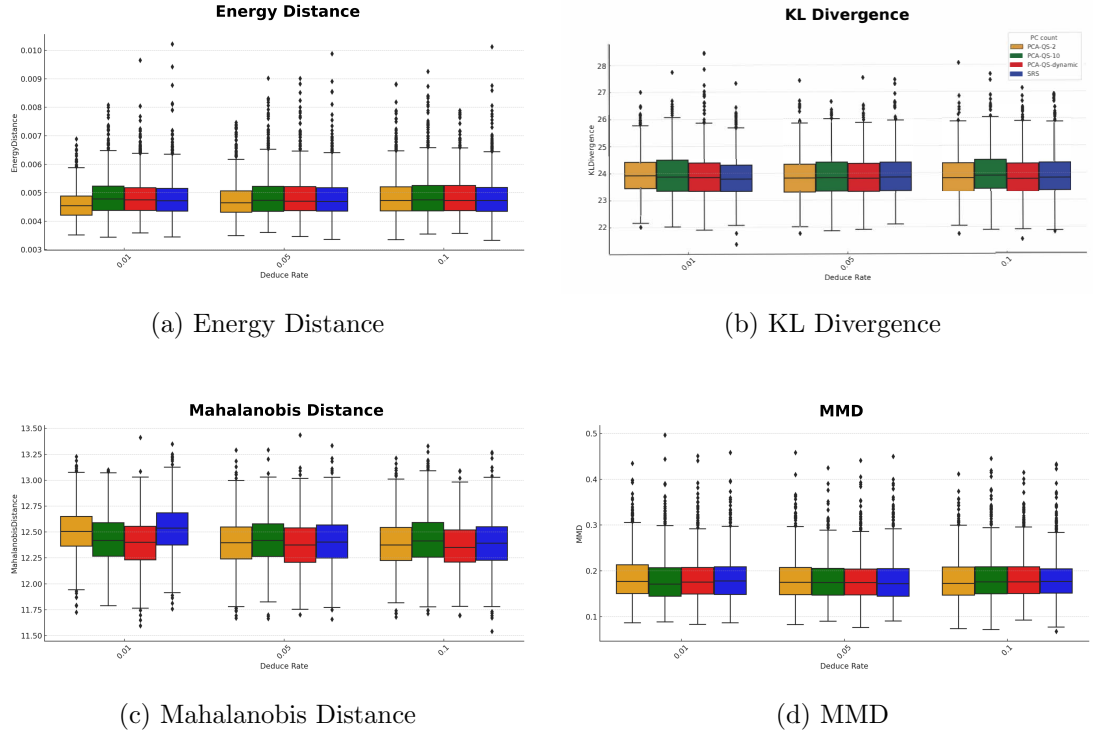


Figure 10: Distance Metrics of Two Sampling Methods with Year Prediction MSD Dataset

3.3.4 Feature Complexity (Text/NLP)

Online News The Online News Popularity dataset from the UCI Machine Learning Repository is a benchmark dataset used to predict the popularity of news articles published on the Mashable website. Each instance in the dataset represents a single news article and includes a set of numerical features that describe the article’s content, metadata, and social engagement metrics. These features cover aspects such as the number of words, presence of images or videos, natural language processing (NLP) indicators, and publication timing. The target variable is the number of times the article was shared on social media, making this a regression problem in its original form, though it is often used for binary classification by thresholding the share count. The dataset contains 39,644 instances and 61 features, all of which are numerical. It provides a rich testbed for predictive modeling, feature selection, and text-driven analytics in the field of digital media and social engagement prediction.

Summary of Real Data Structure-Preserving Comparisons

Across all real-world datasets grouped by class imbalance, time-series nature, scale, and feature complexity, the results consistently show that PCA-QS retains the structural

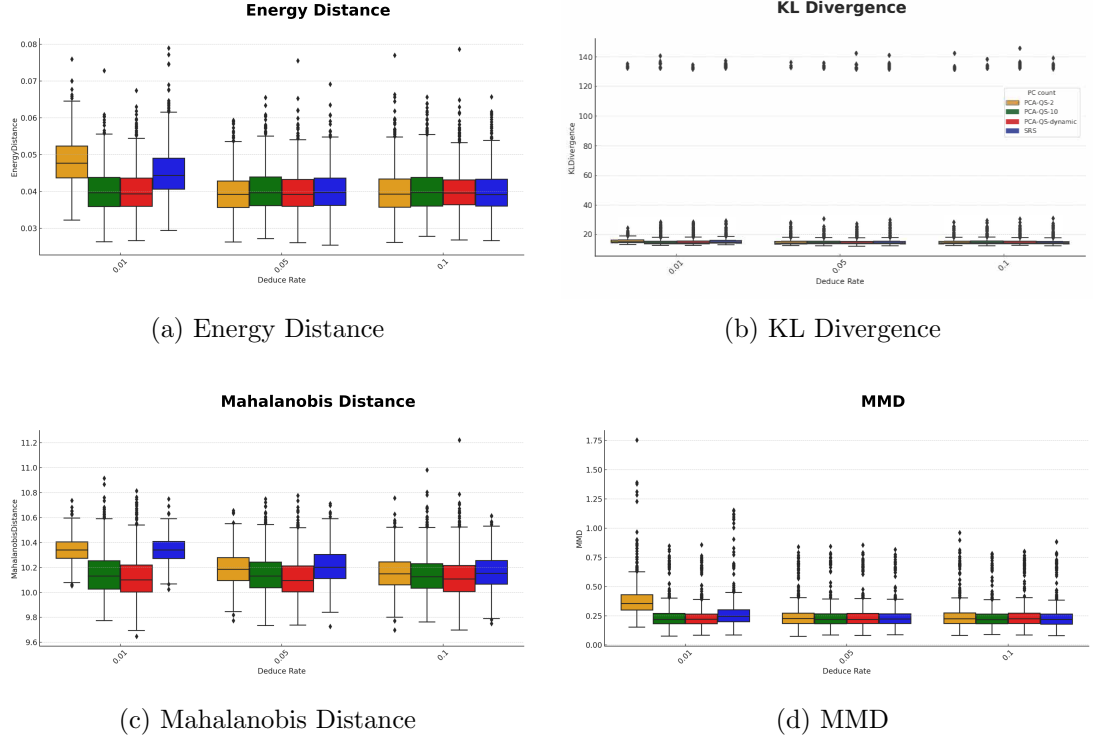


Figure 11: Distance Metrics of Two Sampling Methods with Online News Dataset

and distributional properties of the original datasets more faithfully than Simple Random Sampling (SRS). Specifically, PCA-QS achieves lower Kullback-Leibler divergence, Energy distance, Mahalanobis distance, and Maximum Mean Discrepancy, indicating better alignment in both global and local feature spaces.

This advantage is particularly notable for imbalanced and high-dimensional settings (e.g., CreditCard, MagicGamma), as well as for signal-rich time-series data (EEG, Epileptic Seizure) where local temporal structures are important. Even for massive tabular data (Higgs, YearPredictionMSD) and complex NLP-related features (Online News), PCA-QS demonstrates stable and reliable structure preservation. These findings validate PCA-QS as a robust sampling strategy for downstream analyses where retaining the underlying data geometry is critical.

3.4 Logistic Regression and Other Popular Classification Models

Credit Default Dataset This classification experiment revisits the **Credit Default Dataset** already introduced in the matrix comparison section. Recall that this dataset provides client credit information used to predict whether a payment default will occur.

For model evaluation, we compare **PCA-QS** (with three principal component configurations: `fixed_5`, `fixed_10`, and `dynamic_0.7`) against **SRS** (Simple Random Sampling). The goal is to quantify how well each sampling method preserves predictive structure for supervised learning.

From these experiments, we observe that:

- *AUC Performance*: PCA-QS achieves consistently higher and more stable AUCs than SRS. Dynamic PC and fixed-10 configurations yield the best discrimination.
- *Precision vs. Recall*: SRS occasionally peaks in precision but at the cost of poorer and unstable recall. PCA-QS shows superior balance, crucial for reliable default detection.
- *F1 Score Stability*: PCA-QS, particularly fixed-10, maintains lower variance, indicating robust trade-offs between precision and recall.
- *False Rates and Reliability*: PCA-QS minimizes both false positives and negatives more

consistently than SRS, reducing risk in credit scoring systems.

Table 4: Mean (std) of AUC, F1, Recall, and Precision over 1000 runs for each method/configuration on Credit Default.

Method	PC Config	AUC	F1	Recall	Precision
PCA-QS	Fixed 5	0.9122 (0.0205)	0.5854 (0.0249)	0.8297 (0.0269)	0.4530 (0.0285)
	Fixed 10	0.9691 (0.0050)	0.5974 (0.0114)	0.9143 (0.0069)	0.4438 (0.0124)
	Dynamic =7	0.9807 (0.0008)	0.6048 (0.0050)	0.9256 (0.0026)	0.4492 (0.0055)
SRS	-	0.9055 (0.0221)	0.6112 (0.0321)	0.8113 (0.0289)	0.4918 (0.0401)

Table 5: TPR, TNR, FPR, FNR, and Threshold over 1000 runs for each method on Credit Default.

Method	PC Config	TPR	TNR	FPR	FNR	Threshold
PCA-QS	Fixed 5	0.8297 (0.0269)	0.9758 (0.0029)	0.0242 (0.0029)	0.1703 (0.0269)	0.0148 (0.0008)
	Fixed 10	0.9143 (0.0069)	0.9725 (0.0014)	0.0275 (0.0014)	0.0857 (0.0069)	0.0167 (0.0005)
	Dynamic =7	0.9256 (0.0026)	0.9728 (0.0006)	0.0272 (0.0006)	0.0744 (0.0026)	0.0191 (0.0002)
SRS	-	0.8113 (0.0289)	0.9796 (0.0034)	0.0204 (0.0034)	0.1887 (0.0289)	0.0167 (0.0016)

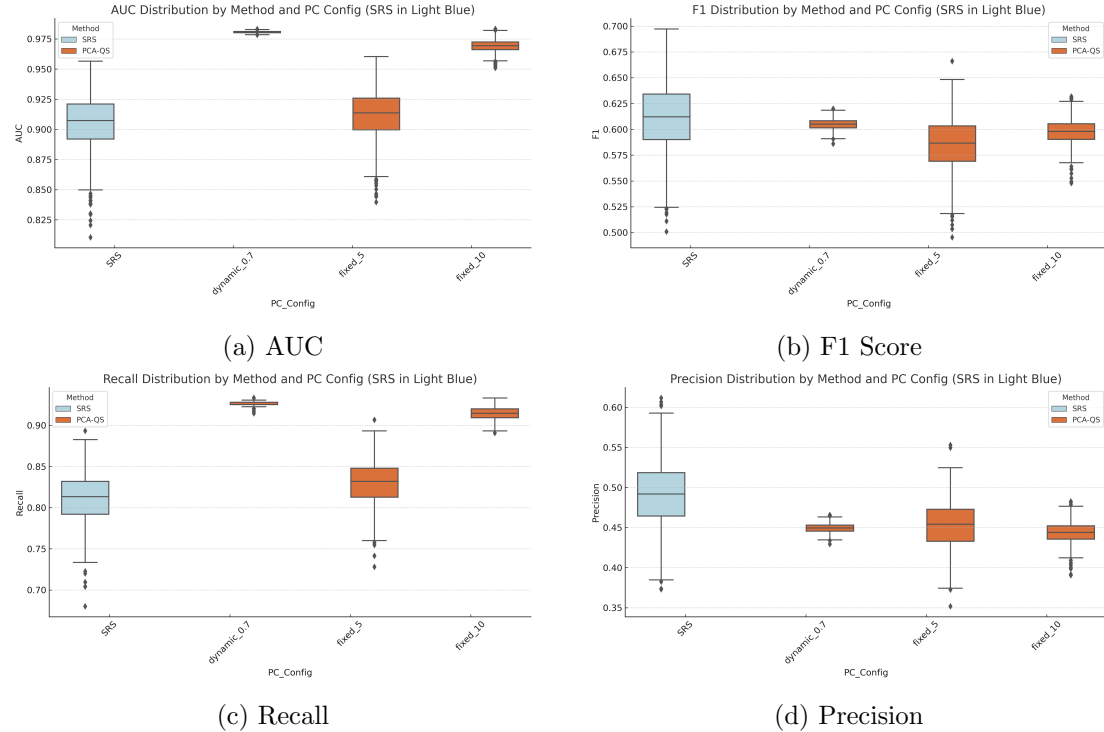


Figure 12: Performance variation across 1000 runs for AUC, F1, Recall, and Precision on Credit Default.

APS Failure at Scania Trucks Dataset The APS Failure dataset was already described in the matrix comparison section; here we revisit it to evaluate classification performance under real-world predictive maintenance. The same three PCA-QS configurations and SRS baseline are compared.

Key observations: - *AUC*: Dynamic and fixed-10 PCA-QS yield highest AUC with minimal variance, outperforming SRS. - *F1 and Recall*: PCA-QS maintains stable F1 and robust recall. SRS shows larger fluctuations, which could lead to missed failures. - *Precision*: SRS sometimes shows slightly higher average precision, but at the expense of lower and unstable recall — risky for fault detection.

Table 6: Mean (std) AUC, F1, Recall, Precision over 1000 runs for APS Failure. Dynamic PCA-QS used actual mean PCs = 21.

Method	PC Config	AUC	F1	Recall	Precision
PCA-QS	Fixed 5	0.9122 (0.0205)	0.5854 (0.0249)	0.8297 (0.0269)	0.4530 (0.0285)
	Fixed 10	0.9691 (0.0050)	0.5974 (0.0114)	0.9143 (0.0069)	0.4438 (0.0124)
	Dynamic =21	0.9807 (0.0008)	0.6048 (0.0050)	0.9256 (0.0026)	0.4492 (0.0055)
SRS	-	0.9055 (0.0221)	0.6112 (0.0321)	0.8113 (0.0289)	0.4918 (0.0401)

Table 7: Average TP, TN, FP, FN, and Threshold for APS over 1000 runs. Dynamic PCA-QS mean PCs = 21.

Method	PC Config	TP	TN	FP	FN	Threshold
PCA-QS	Fixed 5	311.144 (10.0944)	15246.521 (45.4812)	378.479 (45.4812)	63.856 (10.0944)	0.0148 (0.0008)
	Fixed 10	342.879 (2.6041)	15194.624 (22.1261)	430.376 (22.1261)	32.121 (2.6041)	0.0167 (0.0005)
	Dynamic =21	347.117 (0.9676)	15199.247 (9.4625)	425.753 (9.4625)	27.883 (0.9676)	0.0191 (0.0002)
SRS	-	304.227 (10.8334)	15306.375 (53.0452)	318.625 (53.0452)	70.773 (10.8334)	0.0167 (0.0016)

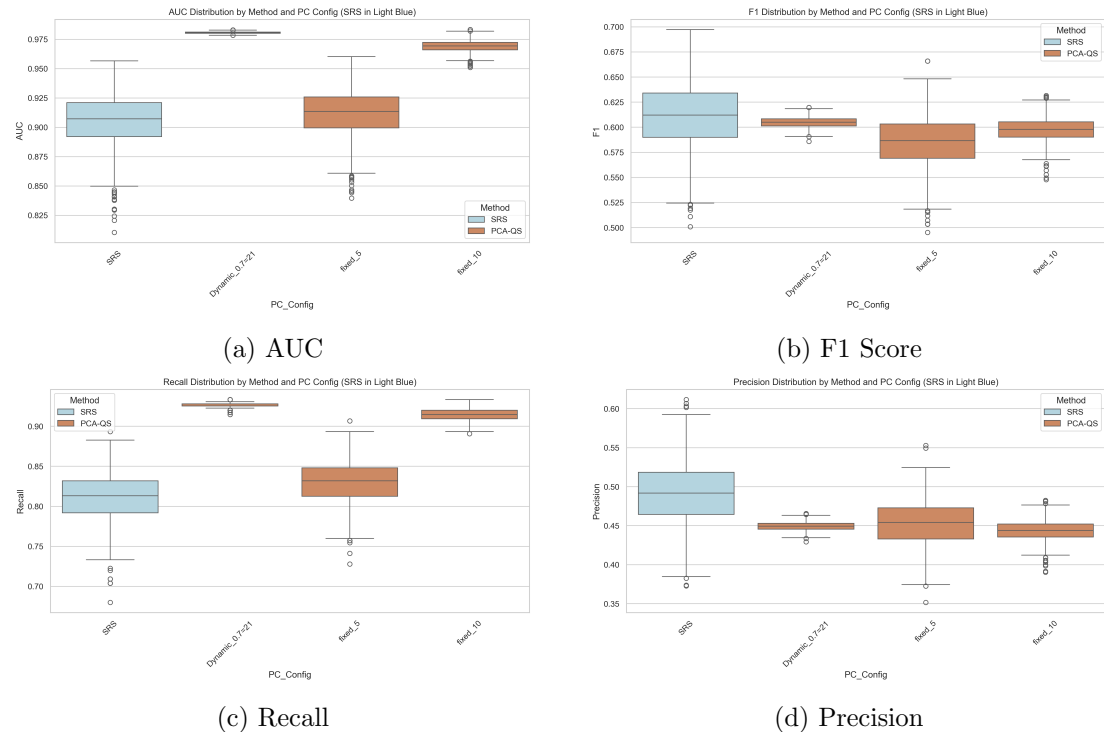


Figure 13: Boxplots comparing PCA-QS and SRS under different PC configurations for APS Failure.

Summary Overall, PCA-QS delivers more reliable and higher classification performance than SRS on both the Credit Default and APS datasets. Dynamic PC configurations consistently maximize AUC and recall with low variance. SRS shows greater variability and less dependable results, reinforcing PCA-QS as the robust choice for practical classification pipelines.

4 Conclusion

This study presents a comprehensive comparative analysis of Principal Component Analysis-guided Quantile Sampling (PCA-QS) and Simple Random Sampling (SRS) methods, evaluated across varying configurations of dimensionality, sample sizes, and principal component counts. The comparison leverages four statistical similarity metrics

— Energy Distance, Maximum Mean Discrepancy (MMD), Mahalanobis Distance, and Kullback–Leibler (KL) Divergence — to quantify the discrepancy between the sampled subsets and the full data distribution. Across all metrics, PCA-QS consistently achieves lower values, indicating superior fidelity in preserving both the statistical and geometric structure of the original dataset. These advantages become more pronounced in higher-dimensional settings and persist across a range of sample sizes and principal component configurations. A composite score aggregating all normalized metrics further confirms the robust performance of PCA-QS. Additionally, clustering analysis delineates specific regimes where SRS performs comparably — typically under low dimensionality and small sample sizes — versus scenarios where PCA-QS offers significant improvements. Overall, the results establish PCA-QS as a robust, scalable, and structure-preserving subsampling method, providing a principled alternative to SRS for large-scale data reduction in modern machine learning workflows.

A Appendix: Detailed Metric Tables

A.1 Imbalanced Datasets

Table 8: UCI Credit Card Dataset

Deduce	Methods	PC	Energy	Mahalanobis	MMD	KLD
0.01	PCA-QS	2	0.0205 (0.0033)	6.3802 (0.1232)	0.2033 (0.0593)	2.0129 (0.3035)
		10	0.0031 (0.0010)	6.1531 (0.1387)	0.0500 (0.0268)	1.0648 (0.2991)
		dynamic	0.0020 (0.0006)	6.1261 (0.1404)	0.0468 (0.0237)	1.0196 (0.2860)
	SRS		0.0213 (0.0057)	6.4039 (0.1228)	0.0996 (0.0508)	2.1145 (0.4257)
		2	0.0039 (0.0006)	6.1850 (0.1417)	0.0441 (0.0187)	1.3388 (0.2620)
		10	0.0031 (0.0010)	6.1526 (0.1417)	0.0507 (0.0264)	1.0653 (0.3043)
		dynamic	0.0021 (0.0005)	6.1346 (0.1470)	0.0464 (0.0245)	1.0326 (0.2998)
	PCA-QS		0.0050 (0.0013)	6.2377 (0.1422)	0.0461 (0.0226)	1.4237 (0.3627)
		2	0.0024 (0.0004)	6.1617 (0.1472)	0.0460 (0.0231)	1.1244 (0.2241)
		10	0.0031 (0.0011)	6.1608 (0.1393)	0.0513 (0.0313)	1.0690 (0.2961)
	SRS		0.0021 (0.0006)	6.1245 (0.1456)	0.0463 (0.0230)	1.0369 (0.2963)
		dynamic	0.0028 (0.0007)	6.2069 (0.1424)	0.0472 (0.0255)	1.1849 (0.3310)

Table 9: MagicGamma Dataset)

Deduce	Sampling	PC	Energy	Mahalanobis	MMD	KLD
0.01	PCA-QS	2	0.0163 (0.0035)	4.1176 (0.0813)	0.0400 (0.0196)	0.3234 (0.0376)
		10	0.0012 (0.0004)	4.0844 (0.0810)	0.0191 (0.0133)	0.0847 (0.0087)
		dynamic	0.0012 (0.0004)	4.0843 (0.0804)	0.0193 (0.0130)	0.0848 (0.0087)
	SRS		0.0211 (0.0079)	4.1306 (0.0844)	0.0611 (0.0408)	0.3123 (0.0498)
		2	0.0031 (0.0007)	4.0936 (0.0853)	0.0137 (0.0077)	0.1548 (0.0181)
		10	0.0012 (0.0005)	4.0847 (0.0799)	0.0185 (0.0117)	0.0852 (0.0087)
	PCA-QS		0.0012 (0.0004)	4.0778 (0.0796)	0.0191 (0.0128)	0.0848 (0.0087)
		2	0.0045 (0.0017)	4.0931 (0.0846)	0.0191 (0.0133)	0.1548 (0.0196)
		10	0.0018 (0.0004)	4.0877 (0.0839)	0.0165 (0.0109)	0.1172 (0.0125)
	SRS		0.0012 (0.0004)	4.0800 (0.0823)	0.0186 (0.0137)	0.0848 (0.0093)
		dynamic	0.0012 (0.0004)	4.0845 (0.0837)	0.0191 (0.0133)	0.0849 (0.0088)
	SRS		0.0025 (0.0009)	4.0874 (0.0819)	0.0190 (0.0126)	0.1186 (0.0133)

A.2 Time-Series and Signal Data

Table 10: EEG Eye State

Deduce	Sampling	PC	Energy	Mahalanobis	MMD	KLD
0.01	PCA-QS	2	0.0961 (0.0137)	3.4933 (0.0902)	5.4727 (0.6681)	3.4852 (3.4786)
		10	0.0007 (0.0003)	4.0189 (0.1355)	0.0274 (0.0322)	3.7867 (3.6362)
		dynamic	0.0005 (0.0002)	4.0086 (0.1385)	0.0262 (0.0309)	3.7882 (3.6250)
	SRS		0.0129 (0.0063)	4.8454 (0.3042)	0.1228 (0.4375)	5.9759 (4.2162)
		2	0.0035 (0.0007)	3.6103 (0.1041)	0.1428 (0.0406)	3.2883 (3.4485)
		10	0.0008 (0.0003)	4.0224 (0.1372)	0.0269 (0.0302)	3.8098 (3.6965)
	PCA-QS		0.0005 (0.0002)	4.0137 (0.1379)	0.0257 (0.0302)	3.9137 (3.8342)
		2	0.0026 (0.0010)	4.6895 (0.4858)	0.0305 (0.0396)	5.6239 (4.1575)
		10	0.0008 (0.0003)	4.0216 (0.1377)	0.0267 (0.0308)	3.8919 (3.6809)
	SRS		0.0005 (0.0002)	4.0105 (0.1345)	0.0266 (0.0309)	3.8287 (3.6640)
		dynamic	0.0014 (0.0005)	4.4867 (0.5523)	0.0284 (0.0320)	5.0408 (3.8959)

Table 11: Epileptic Seizure Dataset

Deduce	Sampling	PC	Energy	Mahalanobis	MMD	KLD
0.01	PCA-QS	2	0.1819 (0.0449)	12.2597 (0.1927)	2.3995 (0.6149)	59.9135 (3.6438)
		10	0.0032 (0.0007)	14.7994 (0.5363)	0.3246 (0.0797)	19.7332 (1.2963)
		dynamic	0.0032 (0.0006)	14.8068 (0.5496)	0.3293 (0.0814)	19.3603 (1.2623)
	SRS	2	0.1241 (0.0264)	12.5550 (0.2385)	1.7178 (0.5595)	61.4068 (3.6020)
		10	0.0257 (0.0038)	14.8048 (0.3930)	0.4883 (0.1239)	45.3470 (2.3583)
		dynamic	0.0033 (0.0006)	14.8170 (0.5080)	0.3233 (0.0806)	19.7411 (1.3099)
0.05	PCA-QS	2	0.0254 (0.0056)	14.7984 (0.5327)	0.3290 (0.0815)	19.4299 (1.2788)
		10	0.0123 (0.0018)	15.8887 (0.4347)	0.3251 (0.0828)	38.2653 (1.8899)
		dynamic	0.0033 (0.0007)	14.7937 (0.5274)	0.3220 (0.0799)	19.6320 (1.2817)
	SRS	2	0.0128 (0.0025)	14.7781 (0.5235)	0.3294 (0.0807)	19.4951 (1.3149)
		10	0.0032 (0.0006)	16.0954 (0.4155)	0.3267 (0.0792)	38.4042 (2.0699)
		dynamic				
0.1	PCA-QS	2	0.0128 (0.0025)	16.0954 (0.4155)	0.3267 (0.0792)	38.4042 (2.0699)
		10				
		dynamic				
	SRS	2				
		10				
		dynamic				

A.3 Large-Scale Tabular Data

Table 12: Higgs Dataset

Deduce	Sampling	PC	Energy	Mahalanobis	MMD	KLD
0.01	PCA-QS	2	0.0048 (0.0007)	7.3007 (0.0728)	0.0531 (0.0160)	5.2867 (0.0664)
		10	0.0028 (0.0005)	7.2976 (0.0758)	0.0545 (0.0179)	4.9860 (0.0600)
		dynamic	0.0028 (0.0005)	7.2970 (0.0729)	0.0556 (0.0186)	4.9819 (0.0586)
	SRS	2	0.0050 (0.0008)	7.3001 (0.0693)	0.0558 (0.0188)	5.2775 (0.0715)
		10	0.0028 (0.0004)	7.2962 (0.0740)	0.0546 (0.0188)	4.9816 (0.0613)
		dynamic	0.0028 (0.0004)	7.2972 (0.0729)	0.0551 (0.0182)	4.9828 (0.0617)
0.05	PCA-QS	2	0.0028 (0.0004)	7.2948 (0.0738)	0.0556 (0.0193)	4.9816 (0.0566)
		10	0.0028 (0.0005)	7.2994 (0.0714)	0.0543 (0.0177)	4.9820 (0.0576)
		dynamic	0.0028 (0.0004)	7.2954 (0.0741)	0.0547 (0.0184)	4.9838 (0.0618)
	SRS	2	0.0028 (0.0004)	7.2963 (0.0732)	0.0547 (0.0175)	4.9812 (0.0600)
		10	0.0028 (0.0005)	7.2949 (0.0767)	0.0546 (0.0180)	4.9810 (0.0566)
		dynamic	0.0028 (0.0005)	7.2944 (0.0734)	0.0547 (0.0183)	4.9874 (0.0607)
0.1	PCA-QS	2	0.0028 (0.0005)	7.2944 (0.0734)	0.0547 (0.0183)	4.9874 (0.0607)
		10				
		dynamic				
	SRS	2				
		10				
		dynamic				

Table 13: Year Prediction MSD Dataset)

Deduce	Sampling	PC	Energy	Mahalanobis	MMD	KLD
0.01	PCA-QS	2	0.0046 (0.0005)	12.5050 (0.2283)	0.1853 (0.0499)	23.9607 (0.7412)
		10	0.0049 (0.0007)	12.4285 (0.2361)	0.1799 (0.0500)	23.9563 (0.8357)
		dynamic	0.0049 (0.0007)	12.3990 (0.2425)	0.1831 (0.0480)	23.9071 (0.8154)
	SRS	2	0.0048 (0.0007)	12.5335 (0.2342)	0.1837 (0.0487)	23.8623 (0.7656)
		10	0.0049 (0.0008)	12.4210 (0.2377)	0.1796 (0.0457)	23.9172 (0.7689)
		dynamic	0.0049 (0.0007)	12.3779 (0.2427)	0.1799 (0.0467)	23.8859 (0.7721)
0.05	PCA-QS	2	0.0048 (0.0006)	12.3958 (0.2368)	0.1825 (0.0486)	23.8851 (0.7591)
		10	0.0049 (0.0008)	12.4120 (0.2377)	0.1796 (0.0457)	23.9172 (0.7689)
		dynamic	0.0049 (0.0007)	12.3779 (0.2427)	0.1799 (0.0467)	23.8859 (0.7721)
	SRS	2	0.0048 (0.0007)	12.4128 (0.2349)	0.1800 (0.0494)	23.9038 (0.7856)
		10	0.0049 (0.0007)	12.3872 (0.2407)	0.1813 (0.0477)	23.8819 (0.7770)
		dynamic	0.0049 (0.0008)	12.4273 (0.2453)	0.1830 (0.0501)	23.9855 (0.8135)
0.1	PCA-QS	2	0.0049 (0.0007)	12.3663 (0.2284)	0.1828 (0.0480)	23.8659 (0.7869)
		10	0.0049 (0.0007)	12.3911 (0.2383)	0.1824 (0.0473)	23.9155 (0.7940)
		dynamic	0.0048 (0.0007)	12.3911 (0.2383)	0.1824 (0.0473)	23.9155 (0.7940)
	SRS	2				
		10				
		dynamic				

A.4 Feature Complexity (Text/NLP)

Table 14: Online News

Deduce	Sampling	PC	Energy	Mahalanobis	MMD	KLD
0.01	PCA-QS	2	0.0482 (0.0061)	10.3405 (0.1006)	0.3796 (0.1371)	16.9013 (12.4243)
		10	0.0402 (0.0059)	10.1516 (0.1707)	0.2372 (0.0975)	16.4014 (13.1539)
		dynamic	0.0401 (0.0060)	10.1190 (0.1740)	0.2361 (0.0963)	16.7481 (14.5030)
	SRS	2	0.0452 (0.0068)	10.3410 (0.1021)	0.2669 (0.1200)	16.8300 (13.0912)
		10	0.0395 (0.0056)	10.1894 (0.1341)	0.2436 (0.1008)	15.4110 (8.6053)
		dynamic	0.0404 (0.0059)	10.1471 (0.1630)	0.2367 (0.0959)	16.1722 (12.4810)
0.05	PCA-QS	2	0.0399 (0.0059)	10.1152 (0.1635)	0.2402 (0.1008)	16.0097 (12.0100)
		10	0.0402 (0.0057)	10.2082 (0.1406)	0.2373 (0.0907)	16.2688 (13.1679)
		dynamic	0.0401 (0.0062)	10.1551 (0.1436)	0.2438 (0.1014)	15.9720 (11.4136)
	SRS	2	0.0401 (0.0061)	10.1394 (0.1584)	0.2344 (0.0920)	15.8864 (10.7884)
		10	0.0401 (0.0059)	10.1198 (0.1668)	0.2464 (0.1083)	16.5685 (14.2315)
		dynamic	0.0399 (0.0059)	10.1630 (0.1391)	0.2371 (0.1021)	16.1921 (12.6247)

References

[Abdi and Williams(2010)] H. Abdi and L. J. Williams. Principal component analysis. *Wiley Interdisciplinary Reviews: Computational Statistics*, 2(4):433–459, 2010.

[Anderson(1963)] T. W. Anderson. *An Introduction to Multivariate Statistical Analysis*. Wiley, 1963.

[Anderson(2003)] T. W. Anderson. *An Introduction to Multivariate Statistical Analysis*. Wiley-Interscience, 2003.

[Atkinson and Donev(1992)] A. Atkinson and A. N. Donev. *Optimum Experimental Designs*. Oxford Science Publications, 1992.

[Bethel(1989)] J. Bethel. *Survey Methods in Community Medicine*. Churchill Livingstone, 1989.

[Bishop(2006)] C. M. Bishop. *Pattern Recognition and Machine Learning*. Springer, 2006.

[Blei et al.(2017)] Blei, Kucukelbir, and McAuliffe] D. M. Blei, A. Kucukelbir, and J. D. McAuliffe. Variational inference: A review for statisticians. *Journal of the American Statistical Association*, 112:859–877, 2017.

[Cadima and Jolliffe(2015)] J. Cadima and I. T. Jolliffe. Principal component analysis: A review and recent developments. *Philosophical Transactions of the Royal Society A*, 374, 2015.

[Cochran(1977)] W. G. Cochran. *Sampling Techniques*. Wiley, 3 edition, 1977.

[Cover and Thomas(2006)] T. M. Cover and J. A. Thomas. *Elements of Information Theory*. Wiley, 2006.

[Cuturi(2013)] M. Cuturi. Sinkhorn distances: Lightspeed computation of optimal transport. *Advances in Neural Information Processing Systems*, 26:2292–2300, 2013.

[Dudley(1999)] Richard M. Dudley. *Uniform Central Limit Theorems*, volume 63 of *Cambridge Studies in Advanced Mathematics*. Cambridge University Press, Cambridge, 1999.

[Filzmoser et al.(2008)] Filzmoser, Maronna, and Werner] P. Filzmoser, R. Maronna, and M. Werner. Outlier detection in high dimensions. *Computational Statistics & Data Analysis*, 52(3):1694–1711, 2008.

[Flamary and Courty(2017)] R. Flamary and N. Courty. Pot: Python optimal transport. *Journal of Machine Learning Research*, 18(170):1–5, 2017.

[Flury(1997)] B. Flury. *A First Course in Multivariate Statistics*. Springer, 1997.

[Frogner et al.(2015)] Frogner, Zhang, Mobahi, Araya, and Poggio] C. Frogner, C. Zhang, H. Mobahi, M. Araya, and T. A. Poggio. Learning with a wasserstein loss. *Advances in Neural Information Processing Systems*, 2015.

[Hastie et al.(2009)] Hastie, Tibshirani, and Friedman] T. Hastie, R. Tibshirani, and J. Friedman. *The Elements of Statistical Learning: Data Mining, Inference, and Prediction*. Springer, 2009.

[Higham(2002)] N. J. Higham. *Accuracy and Stability of Numerical Algorithms*. Society for Industrial and Applied Mathematics, 2002.

[Jackson(1991)] J. E. Jackson. *A User’s Guide to Principal Components*. Wiley, 1991.

[Jobson(2012)] J. D. Jobson. *Applied Multivariate Data Analysis: Volume II: Categorical and Multivariate Methods*. Springer, 2012.

[Johnstone(2001)] I. M. Johnstone. On the distribution of the largest eigenvalue in principal components analysis. *Annals of Statistics*, 29(2):295–327, 2001.

[Jolliffe(1986)] I. T. Jolliffe. *Principal Component Analysis*. Springer, 1986.

[Jolliffe(2016)] I. T. Jolliffe. *Principal Component Analysis*. Springer, 2016.

[Kettenring(2006)] J. R. Kettenring. The practice of mahalanobis distance. *Technometrics*, 2006.

[Kish(1965)] L. Kish. *Survey Sampling*. Wiley, 1965.

[Kullback(1951)] S. Kullback. *Information Theory and Statistics*. John Wiley & Sons, 1951.

[Leemis(1995)] L. M. Leemis. *Reliability: Probabilistic Models and Statistical Methods*. Prentice Hall, 1995.

[Levy and Lemeshow(2008)] P. S. Levy and S. Lemeshow. *Sampling of Populations: Methods and Applications*. Wiley, 2008.

[Lohr(2009)] S. L. Lohr. *Sampling: Design and Analysis*. Brooks/Cole, 2009.

[Lumley(2010)] T. Lumley. *Complex Surveys: A Guide to Analysis Using R*. Wiley, 2010.

[Maesschalck et al.(2000)Maesschalck, Jouan-Rimbaud, and Massart] R. D. Maesschalck, D. Jouan-Rimbaud, and D. L. Massart. The mahalanobis distance. *Chemometrics and Intelligent Laboratory Systems*, 50:1–18, 2000.

[Mardia et al.(1979)Mardia, Kent, and Bibby] K. V. Mardia, J. T. Kent, and J. M. Bibby. *Multivariate Analysis*. Academic Press, 1979.

[Massart(1990)] P. Massart. The tight constant in the dvoretzky-kiefer-wolfowitz inequality. *Annals of Probability*, 18(3):1269–1283, 1990.

[McDonald(2014)] J. H. McDonald. *Handbook of Biological Statistics*. Spicky House Publishing, 2014.

[McLachlan(1999)] G. J. McLachlan. *Mahalanobis Distance*. Wiley, 1999.

[Muirhead(1982)] R. J. Muirhead. *Aspects of Multivariate Statistical Theory*. Wiley, 1982.

[Peyré and Cuturi(2019)] G. Peyré and M. Cuturi. Computational optimal transport. *Foundations and Trends in Machine Learning*, 11(5-6):355–607, 2019.

[Rencher and Christensen(2012)] A. C. Rencher and W. F. Christensen. *Methods of Multivariate Analysis*. Wiley, 2012.

[Santambrogio(2015)] F. Santambrogio. *Optimal Transport for Applied Mathematicians*. Birkhäuser, 2015.

[Searle(2009)] S. R. Searle. *Matrix Algebra Useful for Statistics*. Wiley, 2009.

[Serfling(1980)] R. J. Serfling. *Approximation Theorems of Mathematical Statistics*. Wiley, 1980.

[Shorack and Wellner(1986)] G. R. Shorack and J. A. Wellner. *Empirical Processes with Applications to Statistics*. Wiley, 1986.

[Silverman(1986)] B. W. Silverman. *Density Estimation for Statistics and Data Analysis*. Chapman and Hall, 1986.

[Särndal et al.(2003)] Särndal, Swensson, and Wretman] C.-E. Särndal, B. Swensson, and J. Wretman. *Model Assisted Survey Sampling*. Springer, 2003.

[Thompson(2012)] S. K. Thompson. *Sampling*. Wiley, 3 edition, 2012.

[van der Vaart and Wellner(1996)] A. W. van der Vaart and J. A. Wellner. *Weak Convergence and Empirical Processes*. Springer, 1996.

[Villani(2008)] C. Villani. *Optimal Transport: Old and New*. Springer, 2008.

[Wasserman(2004)] L. Wasserman. *All of Statistics: A Concise Course in Statistical Inference*. Springer, 2004.

[Wickham(2014)] H. Wickham. *Advanced R*. Chapman & Hall/CRC The R Series, 2014.

[Talagrand(1996)] Talagrand, M. (1996). *A new look at independence*. *The Annals of Probability*, 24(1), 1–34.

[Boucheron et al.(2013)] Boucheron, S., Lugosi, G., & Massart, P. (2013). *Concentration Inequalities: A Nonasymptotic Theory of Independence*. Oxford University Press.

[Box(1949)] Box, G. E. P. (1949). *A General Distribution Theory for a Class of Likelihood Criteria*, *Biometrika*, Vol. 36, No. 3/4, pp. 317-346, 1949.